

RG flows on S^d and Hamiltonian truncation

Matthijs Hogervorst

Perimeter Institute for Theoretical Physics, Waterloo, ON, Canada
C.N. Yang Institute for Theoretical Physics, Stony Brook University, USA

Abstract

We describe a nonperturbative method to compute the partition function and correlation functions for scalar QFTs set on the d -dimensional sphere S^d . The method relies on a Hamiltonian picture, where the theory is quantized on S^{d-1} and states evolve in time by means of a time-dependent Hamiltonian. Crucially, the Hilbert space on S^{d-1} is truncated to a finite set of states below a cutoff. Throughout this work we focus on the ϕ^2 and $i\phi^3$ flows in three dimensions. In the first part of this paper we analyze the cutoff-dependence of various observables, computing both divergent and RG-improvement counterterms to be added to the action. Next we present nonperturbative results for the massive scalar on S^3 , finding good agreement in the strong-coupling regime between numerical data and the F -coefficient of the free scalar CFT. We also check that the renormalized $i\phi^3$ theory on S^3 is nonperturbatively UV-finite. The scheme in question breaks the $\text{SO}(d+1)$ spacetime symmetry group of S^d down to $\text{SO}(d)$, and in an example we study how the full symmetry is restored in the continuum limit. The relation between our method and earlier work by Al. B. Zamolodchikov involving a specific RG flow on S^2 is explained as well.

Contents

1	Introduction	3
2	Gaussian theory on S^d	4
2.1	Geometry	4
2.2	Canonical quantization	5
3	Turning on interactions	7
3.1	Hamiltonian picture	7
3.2	Numerical setup and truncation	8
3.3	Discretization error	10
3.4	Other observables	11
3.5	Comparison to Ref. [1]	11
4	Cutoff effects	12
4.1	Covariant results	13
4.2	Leading contribution to the partition function	13
4.3	LO computation for ϕ^2 and ϕ^3 interactions	15
4.4	Antipodal correlation function at (N)LO	16
5	Nonperturbative results	18
5.1	Implementation	18
5.2	ϕ^2 flow on S^3	20
5.3	Cubic interaction	22
6	Ward identities and one-point functions	23
6.1	Operator renormalization at leading order	24
6.2	(N)LO computation for $\langle\phi^2\rangle$	24
7	Discussion	26
A	Spherical harmonics and Gegenbauer polynomials	30
B	Massless integrals	31
C	Additional comments about the algorithm	32

1 Introduction

This paper discusses d -dimensional Euclidean quantum field theories compactified on the sphere S^d . There are various reasons to study QFTs on this specific manifold. For one, the sphere is the only maximally symmetric compact manifold, so it provides a natural setting to study QFTs in finite volume. Second, certain non-local observables on the sphere are natural probes to study the QFT landscape. In two dimensions, the partition function of a QFT on the sphere is related to the c -coefficient, which obeys a famous monotonicity theorem [2] that severely constrains RG flows.¹ More recently, it has been understood that the partition function on S^3 encodes a quantity F that obeys a monotonicity theorem similar to c : specifically, an RG flow between two (unitary) CFTs can only exist if $F_{\text{UV}} > F_{\text{IR}}$ [4].² Unfortunately, it is not known in general how to compute F for general CFTs, and consequently the F -coefficient is only known for theories in certain corners of theory space: see [9–15] for results in free CFTs, CFTs at large N or estimates that were obtained using the epsilon expansion, or [16–19] for theories with extended supersymmetry.

Let us make the relation between the partition function Z_{S^3} and the F -coefficient explicit. Consider any renormalizable QFT, regulated by a local cutoff Λ and put on the sphere with radius R . At large R , the logarithm of the partition function reads

$$\ln Z_{S^3}(R) \underset{R \rightarrow \infty}{\sim} B_1(\Lambda R)^3 + B_2 \Lambda R - F + \dots \quad (1.1)$$

omitting terms that vanish as $R \rightarrow \infty$.³ The dimensionless coefficients $B_{1,2}$ are scheme-dependent and can be set to zero by adding local counterterms to the action (proportional to the cosmological constant and the Ricci scalar). Predicting F for e.g. the 3d Ising CFT therefore requires computing $Z_{S^3}(R)$ for the ϕ^4 theory with a fine-tuned mass term at large values of R , and subtracting the two terms with coefficients $B_{1,2}$. Since any RG flow initiated by a relevant operator is strongly coupled at large R , it follows that the above computation can only be performed using nonperturbative methods.

It is therefore an interesting exercise to develop algorithms that allow for efficient QFT computations on S^3 , or more generally on S^d . In principle, it is possible to perform Monte Carlo simulations on any latticized manifold with curvature. In practice, this is rather challenging: special care must be taken in order to guarantee that the QFT in question has the correct continuum limit as the lattice spacing is sent to zero. In recent years, Brower et al. [21–23] have made significant progress towards solving this problem and developing Monte Carlo algorithms for QFTs on S^2 and $\mathbb{R} \times S^2$. For earlier work in the same vein, we point to Refs. [24–26].

In the present work a different approach is taken, based on the philosophy of Hamiltonian truncation. This is a variational approach to quantum field theory, see e.g. [27] for a review of the subject and Refs. [28–41] for some recent examples. Concretely we consider d -dimensional scalar QFTs with polynomial interactions

$$S[\phi] = S_0[\phi] + \sum_n \frac{\lambda_n}{n!} \int_{S^d} \sqrt{g} d^d x \phi^n(x) \quad (1.2)$$

where $S_0[\phi]$ is a Gaussian action (including a curvature coupling $\propto \mathcal{R}\phi^2$). We proceed by canonically quantizing ϕ with respect to a foliation of S^d that has S^{d-1} timeslices. This means that we treat the theory (1.2) as an quantum system in $d-1$ dimensions with a time-dependent Hamiltonian. Instead of working with the full Fock space of the theory, we restrict to a large but finite number of states, characterized by a hard cutoff Λ . After this truncation, it is possible to compute observables like the partition function nonperturbatively, and the exact answer is recovered by taking the continuum limit

¹See also [3] for an attempt to generalize the c -theorem to $d > 2$ dimensions.

²Often, the same quantity F is discussed in the context of entanglement entropy, see e.g. [5–8].

³See Ref. [20] for a pedagogical discussion.

$\Lambda \rightarrow \infty$. Our approach differs from most of the Hamiltonian truncation literature, where QFTs on manifolds of the form $\mathbb{R} \times \mathcal{M}$ are considered. In such cases, “solving” the QFT amounts to estimating the spectrum of its Hamiltonian on \mathcal{M} (or the transfer matrix, in the case of spin systems).

One interesting theory to study in this setting is the ϕ^2 RG flow, i.e. the massive boson on S^d . Since this theory is exactly solvable, it serves as a benchmark, where numerical data can be compared to analytic results. A second theory of interest is the ϕ^3 interaction with imaginary coupling.⁴ Although the $i\phi^3$ theory is non-unitary, it provides a simple example of an interacting QFT in $d > 2$. Many generic features of $d > 2$ RG flows (notably UV divergences) are already present in this model. It is possible to flow from the free theory with an $i\phi^3$ interaction to the Yang-Lee CFT, but reaching the critical point requires a UV finetuning, and this is left for future work.

This paper is organized as follows. In Sec. 2 we define a specific foliation of S^d that will be used to quantize the scalar field ϕ on S^d . In Sec. 3, an explicit procedure to compute the partition function and certain correlation functions is described, and the method in question is compared to earlier work involving minimal model flows on S^2 . All observables measured in this scheme depend on the cutoff Λ ; in Sec. 4 this cutoff-dependence will be studied in perturbation theory, and various counterterms that are generated are computed. In Sec. 5, the method is tested numerically, for both the ϕ^2 and $i\phi^3$ theories on S^3 . Finally, the breaking of $\text{SO}(d+1)$ at the cutoff scale is examined in Sec. 6.

2 Gaussian theory on S^d

In this section we will discuss the canonical quantization of a non-interacting scalar theory on S^d . We start by defining a foliation of S^d , and proceed by explicitly developing the necessary canonical quantization.

2.1 Geometry

The foliation of S^d used in this paper is defined as follows. We take the leafs (or timeslices) to be parallel copies of S^{d-1} , parametrized by a spherical coordinate \mathbf{n} . The remaining Euclidean time coordinate is denoted as $\tau \in \mathbb{R}$. Explicitly, we define $S^d \subset \mathbb{R}^{d+1}$ by means of the following parametrization:

$$X^\mu(\tau, \mathbf{n}) = \frac{R}{\cosh \tau} (\sinh \tau, \mathbf{n}) \in \mathbb{R}^{d+1}, \quad \delta_{\mu\nu} X^\mu X^\nu = R^2. \quad (2.1)$$

The points $\tau = \pm\infty$ correspond to the North and South poles of S^d , whereas $\tau = 0$ parametrizes the equator. A sketch of this foliation is shown in Fig. 1. In the coordinates of (2.1) the induced metric on S^d reads

$$ds^2 = \left(\frac{R}{\cosh \tau} \right)^2 [d\tau^2 + d\Omega(\mathbf{n})^2] \quad (2.2)$$

where $d\Omega(\mathbf{n})^2$ is the standard metric of a unit-radius S^{d-1} . In particular, Eq. (2.2) exhibits that the sphere is topologically equivalent to the d -dimensional cylinder $\mathbb{R} \times S^{d-1}$.

Let us proceed by stating some technical results that will be necessary in the rest of this paper. First, we recall that the scalar curvature of the sphere is constant and given by $\mathcal{R} = d(d-1)/R^2$. In the (τ, \mathbf{n}) coordinates, the Laplacian on S^d is given by

$$\nabla^2 = \left(\frac{\cosh \tau}{R} \right)^2 \left[\frac{\partial^2}{\partial \tau^2} - (d-2) \tanh \tau \frac{\partial}{\partial \tau} - \tilde{L}^2 \right]. \quad (2.3)$$

⁴The ϕ^3 theory with real coupling in d dimensions does not exist nonperturbatively. The same theory with imaginary coupling has a \mathcal{PT} symmetry [42] that makes the theory well-defined.

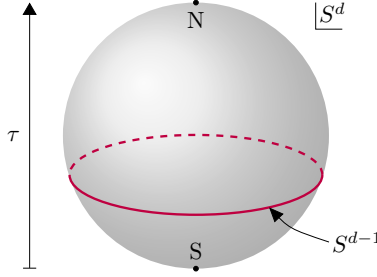


Figure 1: Foliation of S^d where every leaf is a copy of S^{d-1} . Euclidean time $\tau \in \mathbb{R}$ runs upwards from the South to the North pole, with $\tau = 0$ describing the equator.

Here \vec{L}^2 is the positive Laplacian on S^{d-1} , having eigenvalues $\ell(\ell + d - 2)$.⁵ The multiplicity of the ℓ -th eigenvalue is

$$n_\ell^d = \frac{(2\ell + d - 2)(\ell + d - 3)!}{\ell!(d - 2)!}, \quad \ell = 0, 1, 2, \dots \quad (2.4)$$

and we denote the corresponding eigenfunctions — the (hyper)spherical harmonics — by $Y_{\ell j}(\mathbf{n})$. We refer to Appendix A for the conventions used in this paper and some useful identities..

The isometry group of the d -sphere is $\text{SO}(d + 1)$, contrasting with the Poincaré group (or its Euclidean counterpart) in flat space. A subgroup $\text{SO}(d) \subset \text{SO}(d + 1)$ acts only on the spatial coordinate \mathbf{n} . The remaining d generators mix space and time, and are the counterpart of the generators P_μ of translations in flat space. We stress that the generator of time translations $\partial/\partial\tau$ is *not* a Killing vector, which means that there is no notion of (conserved) energy. Physically, the isometries of S^d impose nontrivial constraints on correlation functions [44]. If we consider a correlator of n scalar operators \mathcal{O}_i , these constraints take the form of Ward identities:

$$\sum_{i=1}^n L_a^{(i)} \cdot \langle \mathcal{O}_1(\tau_1, \mathbf{n}_1) \cdots \mathcal{O}_n(\tau_n, \mathbf{n}_n) \rangle = 0 \quad (2.5)$$

where $L_a^{(i)}$ is a first-order differential operator acting on the insertion $\mathcal{O}_i(\tau_i, \mathbf{n}_i)$. There is one such equation for every generator L_a of $\text{SO}(d + 1)$. For $n = 1$, the constraint (2.5) implies that every scalar one-point function $\langle \mathcal{O}(\tau, \mathbf{n}) \rangle$ is constant on S^d . Two-point functions may only depend on the *chordal distance* \mathcal{S} between two points:

$$\langle \mathcal{O}_1(\tau_1, \mathbf{n}_1) \mathcal{O}_2(\tau_2, \mathbf{n}_2) \rangle = f(\mathcal{S}) \quad (2.6)$$

where f is an arbitrary function and

$$\mathcal{S} := \frac{1}{(2R)^2} \|X^\mu(\tau_1, \mathbf{n}_1) - X^\mu(\tau_2, \mathbf{n}_2)\|^2 = \frac{\cosh(\tau_1 - \tau_2) - \mathbf{n}_1 \cdot \mathbf{n}_2}{2 \cosh \tau_1 \cosh \tau_2}. \quad (2.7)$$

By construction, \mathcal{S} is invariant under $\text{SO}(d + 1)$ transformations and bounded: $0 \leq \mathcal{S} \leq 1$. More complicated constraints apply to correlators of $n > 2$ operators and spinning correlators, but such Ward identities will not play a role in the present work.

2.2 Canonical quantization

Let us proceed by setting up the canonical quantization of a scalar field in $d \geq 2$ dimensions with respect to the foliation described in Sec. 2.1. As a starting point, consider the conformally coupled

⁵See [43] for a comprehensive discussion of this operator.

scalar boson, described by the following action:

$$S_0[\phi] = \frac{1}{2} \int_{S^d} \sqrt{g} d^d x [g^{\mu\nu} \partial_\mu \phi \partial_\nu \phi + \xi_c \mathcal{R} \phi^2 + m^2 \phi^2], \quad \xi_c = \frac{d-2}{4(d-1)}. \quad (2.8)$$

By construction the above action is conformally invariant if $m^2 = 0$, although we will keep the bare mass m general for now. Working in arbitrary coordinates x^μ , the $\langle \phi(x_1) \phi(x_2) \rangle$ two-point function is the unique solution to the Klein-Gordon equation

$$[-\nabla_{x_1}^2 + \xi_c \mathcal{R} + m^2] \langle \phi(x_1) \phi(x_2) \rangle = \frac{\delta^{(d)}(x_1, x_2)}{\sqrt{g(x_1)}} \quad (2.9)$$

that is regular on S^d , away from the coincident limit $x_1 \rightarrow x_2$. The solution can be written in compact form as

$$\begin{aligned} \langle \phi(\tau_1, \mathbf{n}_1) \phi(\tau_2, \mathbf{n}_2) \rangle &= \frac{1}{R^{d-2}} \frac{S_d}{2(2\pi)^d} \Gamma(\tfrac{1}{2}(d-1) + \zeta) \Gamma(\tfrac{1}{2}(d-1) - \zeta) \\ &\times \frac{1}{\mathcal{S}^{\frac{1}{2}d-1}} {}_2F_1(\tfrac{1}{2} + \zeta, \tfrac{1}{2} - \zeta; \tfrac{1}{2}d; 1 - \mathcal{S}), \quad \zeta := \sqrt{\tfrac{1}{4} - m^2 R^2}. \end{aligned} \quad (2.10)$$

Here $S_d := \text{vol}(S^{d-1}) = 2\pi^{\frac{1}{2}d}/\Gamma(\frac{1}{2}d)$ and \mathcal{S} is the chordal distance introduced in Eq. (2.7). Notice that depending on the value of m , ζ is either real or purely imaginary; nonetheless, the Green's function (2.10) is manifestly real, since it is invariant under $\zeta \mapsto -\zeta$.

At the same time, the action (2.8) can be quantized using a well-known recipe [45]. We will leave the details of this computation to the reader and merely state the results. The mode decomposition of ϕ is given by

$$\phi(\tau, \mathbf{n}) = \frac{1}{R^{\frac{1}{2}d-1}} \sum_{\ell=0}^{\infty} \sum_{j=1}^{n_\ell^d} a_{\ell j} K_\ell(\tau) Y_{\ell j}(\mathbf{n}) + a_{\ell j}^\dagger K_\ell(-\tau) Y_{\ell j}^*(\mathbf{n}) \quad (2.11)$$

where the $K_\ell(\tau)$ are certain mode functions, to wit:

$$\begin{aligned} K_\ell(\tau) &= \frac{\sqrt{\tfrac{1}{2}\Gamma(\ell + \tfrac{1}{2}(d-1) + \zeta)\Gamma(\ell + \tfrac{1}{2}(d-1) - \zeta)}}{\Gamma(\ell + \tfrac{1}{2}d)} \\ &\times (\cosh \tau)^{\frac{1}{2}d-1} e^{-(\ell + \frac{1}{2}d-1)\tau} {}_2F_1\left[\begin{matrix} \frac{1}{2} + \zeta, \frac{1}{2} - \zeta \\ \ell + \frac{1}{2}d \end{matrix} \middle| \frac{1 - \tanh \tau}{2}\right]. \end{aligned} \quad (2.12)$$

The creation and annihilation operators in (2.11) obey canonical commutation relations:

$$[a_{\ell j}, a_{\ell' j'}^\dagger] = \delta_{\ell\ell'} \delta_{jj'}, \quad [a_{\ell j}, a_{\ell' j'}] = [a_{\ell j}^\dagger, a_{\ell' j'}^\dagger] = 0. \quad (2.13)$$

Using Eq. (2.3), it can easily be checked that (2.11) is a solution to the Klein-Gordon equation. Remark that the field ϕ defined in (2.11) is Hermitian in the Euclidean sense, meaning that ϕ obeys

$$\phi(\tau, \mathbf{n})^\dagger = \phi(-\tau, \mathbf{n}). \quad (2.14)$$

The mode decomposition (2.11) can be checked by computing the time-ordered two-point function of ϕ inside the Fock space vacuum $|\emptyset\rangle$ and comparing the result to (2.10). This yields

$$\begin{aligned} \langle \emptyset | T \phi(\tau_1, \mathbf{n}_1) \phi(\tau_2, \mathbf{n}_2) | \emptyset \rangle &= \frac{1}{R^{d-2}} \sum_{\ell=0}^{\infty} \frac{n_\ell^d}{S_d} C_\ell^d(\mathbf{n}_1 \cdot \mathbf{n}_2) \left[\Theta(\tau_1 > \tau_2) K_\ell(\tau_1) K_\ell(-\tau_2) \right. \\ &\quad \left. + \Theta(\tau_2 > \tau_1) K_\ell(\tau_2) K_\ell(-\tau_1) \right] \end{aligned} \quad (2.15)$$

where the $C_\ell^d(z)$ denote d -dimensional Gegenbauer polynomials, as defined in Appendix A. Both expressions agree, as can for instance be checked numerically.

It is straightforward to define composite operators, provided that one normal-orders all creation and annihilation operators in the relevant mode decompositions. For instance, the operator $:\phi^n:$ is defined as

$$:\phi^n(\tau, \mathbf{n}): = \sum_{k=0}^n \binom{n}{k} \phi_+^k(\tau, \mathbf{n}) \phi_-^{n-k}(\tau, \mathbf{n}) \neq [\phi(\tau, \mathbf{n})]^n \quad (2.16)$$

where ϕ_+ (resp. ϕ_-) denotes the part of ϕ containing creation (annihilation) operators. Since we will always normal-order composite operators, we will omit the $:\mathcal{O}:$ notation from now on and write \mathcal{O} instead. Time-ordered correlation functions of composite operators can be computed using the canonical commutation relations, similar to (2.15).

3 Turning on interactions

Next, let us turn our attention to interacting scalar theories. We start by expressing the partition function of an interacting QFT in terms of a time-evolution operator U . We then discuss a method to systematically approximate this operator in detail.

3.1 Hamiltonian picture

Let us consider a general interacting QFT, e.g. having an action of the form (1.2). More generally, we consider an exactly solvable theory S_0 , either a Gaussian theory or a CFT, that is perturbed by a local operator \mathcal{O} :

$$S = S_0 + \delta S, \quad \delta S = \lambda \int_{S^d} \sqrt{g} d^d x \mathcal{O}(x). \quad (3.1)$$

We assume that \mathcal{O} is relevant, meaning that we can assign a scaling dimension $\Delta < d$ to \mathcal{O} , and the coupling λ has mass dimension $[\lambda] = d - \Delta$. Working in the (τ, \mathbf{n}) coordinates from Sec. 2.1, we can rewrite the interaction term (3.1) as

$$\delta S = \bar{\lambda} \int_{\mathbb{R}} \frac{d\tau}{(\cosh \tau)^d} \hat{\mathcal{O}}(\tau) \quad \text{where} \quad \hat{\mathcal{O}}(\tau) := R^\Delta \int_{S^{d-1}} d\mathbf{n} \mathcal{O}(\tau, \mathbf{n}) \quad (3.2)$$

and $\bar{\lambda}$ denotes the dimensionless coupling $\bar{\lambda} \equiv \lambda R^{d-\Delta}$. In the path integral picture, the partition function of the interacting theory is given by

$$Z(\lambda) = \int [d\phi] e^{-S_0 - \delta S}. \quad (3.3)$$

In principle, Eq. (3.3) can be expressed as an infinite sum of integrated correlation functions in the $\lambda = 0$ theory. Explicitly:

$$Z(\lambda) = \sum_{n=0}^{\infty} \frac{(-\bar{\lambda})^n}{n!} \prod_{i=1}^n \int_{-\infty}^{\infty} \frac{d\tau_i}{(\cosh \tau_i)^d} \langle \hat{\mathcal{O}}(\tau_1) \cdots \hat{\mathcal{O}}(\tau_n) \rangle_0 Z(0). \quad (3.4)$$

The notation $\langle \mathcal{X} \rangle_0$ denotes correlators that are measured in the free theory, i.e.

$$\langle \mathcal{X} \rangle_0 = \frac{1}{Z(0)} \int [d\phi] \mathcal{X} e^{-S_0} \quad (3.5)$$

where \mathcal{X} is any string of local operators. As is customary, we can work with time-ordered correlators instead:

$$\frac{Z(\lambda)}{Z(0)} = \sum_{n=0}^{\infty} (-\bar{\lambda})^n \prod_{i=1}^n \int_{\tau_i < \tau_{i+1}} \frac{d\tau_i}{(\cosh \tau_i)^d} \langle \hat{\mathcal{O}}(\tau_n) \cdots \hat{\mathcal{O}}(\tau_1) \rangle_0 \quad (3.6)$$

at the expense of omitting the $1/n!$ factor appearing in Eq. (3.4). Expressions like (3.6) are ubiquitous in the interaction picture of quantum mechanics. To proceed, we interpret the correlation functions in (3.6) as matrix elements, cf. the discussion from the previous section:

$$\langle \hat{\mathcal{O}}(\tau_n) \cdots \hat{\mathcal{O}}(\tau_1) \rangle_0 = \langle \emptyset | T \hat{\mathcal{O}}(\tau_1) \cdots \hat{\mathcal{O}}(\tau_n) | \emptyset \rangle. \quad (3.7)$$

Then the RHS of (3.6) can then be interpreted as a matrix element of a time-evolution operator U , to wit:

$$\boxed{\frac{Z(\lambda)}{Z(0)} = \langle \emptyset | U(\infty, -\infty) | \emptyset \rangle, \quad U(\tau_f, \tau_i) = T \exp \left[-\bar{\lambda} \int_{\tau_i}^{\tau_f} \frac{d\tau}{(\cosh \tau)^d} \hat{\mathcal{O}}(\tau) \right].} \quad (3.8)$$

In quantum mechanics, U is often referred to as a *Dyson operator*.

At a first glance, Eq. (3.8) seems to be nothing but a rewriting of the perturbative expansion (3.4). In practice, the above formula provides a powerful way to evaluate $Z(\lambda)$ numerically. The basic idea is to divide the sphere into many timeslices. Concretely, given any two times $\tau_i < \tau_f$ we can write the Dyson operator on the interval $[\tau_i, \tau_f]$ as

$$U(\tau_f, \tau_i) = \prod_{k=0}^{T-1} U(\tau_k + \tfrac{1}{2}\delta\tau, \tau_k - \tfrac{1}{2}\delta\tau), \quad \tau_k = \tau_i + (k + \tfrac{1}{2})\delta\tau, \quad (3.9)$$

where $\delta\tau \equiv (\tau_f - \tau_i)/T$. The product in (3.9) runs from right to left, i.e. $k = 0$ (resp. $k = T - 1$) is the rightmost (leftmost) factor. Note that the formula (3.9) is exact, regardless of the number of timeslices T .

A second important idea is that for sufficiently large T , every individual factor in (3.9) can be replaced by a first-order approximation in $\delta\tau$. Crucially, this approximation induces an error of order $1/T$, hence the operator $U(\tau_f, \tau_i)$ is recovered in the limit $T \rightarrow \infty$. Quantitatively, this statement can be phrased as the following identity

$$U(\tau_f, \tau_i) = \prod_{k=0}^{T-1} \left[\mathbb{1} - \frac{\bar{\lambda}\delta\tau}{(\cosh \tau_k)^d} \hat{\mathcal{O}}(\tau_k) \right] + O(1/T) \quad (3.10)$$

which is known as a *Trotter* or *Suzuki-Trotter formula*. A simple derivation of this result will be given in Sec. 3.3. In the next section, we will explain how formula (3.10) can be used in practice to compute $Z(\lambda)$.

3.2 Numerical setup and truncation

The Trotter formula (3.10) provides a starting point for a numerical evaluation of matrix elements of U . Every individual factor in this formula involves an infinite-dimensional operator $\hat{\mathcal{O}}(\tau)$. In the scalar theories studied in this paper, these operators act on the Fock space \mathcal{F} of creation operators $a_{\ell j}^\dagger$. Between every two factors in (3.10), a resolution of the identity can be inserted: if

$$u(\tau) := \mathbb{1} - \frac{\bar{\lambda}\delta\tau}{(\cosh \tau)^d} \hat{\mathcal{O}}(\tau) \quad (3.11)$$

then

$$u(\tau_{k+1})u(\tau_k) = \sum_{|\psi\rangle \in \mathcal{F}} u(\tau_{k+1})|\psi\rangle\langle\psi|u(\tau_k) \quad (3.12)$$

assuming that the states $|\psi\rangle$ form an orthonormal basis of \mathcal{F} . By using (3.12) repeatedly, the Trotter formula reduces the computation of the partition function to an expression involving an infinite number of matrix elements $\langle\psi_i|\hat{\mathcal{O}}(\tau)|\psi_j\rangle$. In the present work, we instead truncate to a finite subset of states $\mathcal{F}(\Lambda) \subset \mathcal{F}$ depending on a UV cutoff Λ to be defined later. Instead of the resolution of the identity in (3.12), we therefore use the approximation

$$u(\tau_{k+1})u(\tau_k) \longrightarrow u(\tau_{k+1})P_\Lambda u(\tau_k), \quad P_\Lambda = \sum_{|\psi\rangle \in \mathcal{F}(\Lambda)} |\psi\rangle\langle\psi|. \quad (3.13)$$

The subspace $\mathcal{F}(\Lambda)$ consists of all states with a certain “energy” $E(|\psi\rangle) \leq \Lambda$. The term energy is a misnomer, since there is no notion of energy on S^d , but with a slight abuse of language we will use this term from now on. To define E , it is necessary to organize the Fock space into basis states of the following form

$$|\psi\rangle = \sum_{\{j_i\}} T_\psi^{j_1 \dots j_n} a_{\ell_1 j_1}^\dagger \dots a_{\ell_n j_n}^\dagger |\emptyset\rangle \quad (3.14)$$

where T_ψ is a tensor with labels in the (symmetrized) $\ell_1 \otimes \dots \otimes \ell_n$ representation of $\text{SO}(d)$. For a state of the form (3.14), the energy $E(|\psi\rangle)$ is defined as follows:⁶

$$E(|\psi\rangle) = \sum_{i=1}^n \varepsilon(\ell_i), \quad \varepsilon(\ell) = \sqrt{\ell(\ell + d - 2)/R^2 + m^2 + d(d - 2)/(4R^2)}. \quad (3.15)$$

Roughly speaking, $\varepsilon(\ell)$ measures the single-particle energy of a spin- ℓ mode, measured at the equator. Indeed, the operator $D = -\nabla^2 + m^2 + \xi_c \mathcal{R}$ acts on spherical harmonics as

$$D \cdot Y_{\ell j}(\mathbf{n}) = [(\cosh \tau)^2 \ell(\ell + d - 2)/R^2 + m^2 + \xi_c \mathcal{R}] Y_{\ell j}(\mathbf{n}).$$

The quantity inside brackets equals $\varepsilon(\ell)^2$ at $\tau = 0$ and is strictly larger for all other τ . Clearly, there are many other possible ways to truncate the Fock space, and perhaps a different truncation procedure is more efficient. We leave this question open for future work.

Summarizing, there are two different cutoffs used in this work, Λ and T . The former has a simple physical interpretation: it is a hard cutoff in energy, which means that correlation functions can only be resolved up to timescales $\Delta\tau \gtrsim 1/\Lambda R$. On the other hand, the number of timeslices T is an unphysical regulator that only controls the discretization error in the Trotter formula (3.10).

So far, we have glanced over one important detail. In Eqs. (3.9) and (3.10), we chose the sampling times $\{\tau_k\}$ uniformly over the interval $[\tau_i, \tau_f]$. Such a uniform sampling is not feasible in practice, since the endpoints τ_f, τ_i must be sent to $\pm\infty$ when the partition function is measured. Rather, we introduce a new time coordinate $z = z(\tau) \in [0, 1]$ as follows

$$z(\tau) := \frac{S_d}{S_{d+1}} \int_{-\infty}^{\tau} \frac{d\tau'}{(\cosh \tau')^d} \quad (3.16)$$

and from now on we will sample uniformly in z . To be completely explicit, this means that Trotter formulas like Eq. (3.10) will be evaluated at times $z_k = (k + \frac{1}{2})/T$ for $k = 0, 1, \dots, T - 1$. In order not to overload the notation, we will mostly use the notation τ instead of z throughout this paper.

⁶For $d = 2$, the truncated Hilbert space $\mathcal{F}(\Lambda)$ is only finite if $m^2 > 0$. For $d > 2$, $\mathcal{F}(\Lambda)$ is always finite.

3.3 Discretization error

In this section, we will present a heuristic derivation of the Trotter formula (3.10). Keeping the UV cutoff Λ fixed, we will argue that the discretization error in (3.10) vanishes as $1/T$ in the limit $T \rightarrow \infty$, although the Trotter formula applies to a more general class of operators [46]. This derivation is unimportant for the rest of this work, and can be skipped on a first reading.

After truncating, the operators $U(\tau', \tau)$ and $\hat{\mathcal{O}}(\tau)$ are matrices that act on the finite-dimensional vector space $\mathcal{F}(\Lambda)$. Let $\|\cdot\|$ denote the L_2 norm on the space of such matrices, $\|\mathcal{O}\|^2 = \text{tr } {}^t\mathcal{O}\mathcal{O}$. On a sufficiently small interval of size $\delta\tau$, the error made using the Trotter approximation can be bounded as follows:

$$\begin{aligned} \left\| U(\tau + \tfrac{1}{2}\delta\tau, \tau - \tfrac{1}{2}\delta\tau) - \left(\mathbb{1} - \frac{\bar{\lambda}\delta\tau}{(\cosh \tau)^d} \hat{\mathcal{O}}(\tau) \right) \right\| \\ \leq \frac{1}{2} \frac{\bar{\lambda}^2 \delta\tau^2}{(\cosh \tau)^{2d}} \|\hat{\mathcal{O}}(\tau)\|^2 + \bar{\lambda} \delta\tau^2 \left\| \frac{d}{d\tau} \frac{\hat{\mathcal{O}}(\tau)}{(\cosh \tau)^d} \right\| + O(\delta\tau^3). \end{aligned} \quad (3.17)$$

The first term on the RHS of (3.17) originates from replacing the function $\exp(\cdot)$ appearing in the evolution operator U by its linearization. The second term arises because \mathcal{O} is evaluated at time τ , instead of integrating over the interval $[\tau - \frac{1}{2}\delta\tau, \tau + \frac{1}{2}\delta\tau]$. A precise estimate of either of these terms is not important. However, for definiteness, we find that for operators $\mathcal{O} = \phi^n$ in $d = 3$, there exists a rough bound of the following form:

$$d = 3: \quad \|\widehat{\phi^n}(\tau)\| \lesssim b(\cosh \tau)^{n/2} \exp(c\Lambda^{2/3}), \quad b, c = O(1). \quad (3.18)$$

The $\exp(c\Lambda^{2/3})$ growth reflects the number of states below the cutoff (i.e. the size of the matrix $\hat{\mathcal{O}}(\tau)$). Likewise, a precise bound on the second term will not be important, but a rough estimate gives

$$\left\| \frac{d}{d\tau} \hat{\mathcal{O}}(\tau) \right\| \lesssim \Lambda \|\hat{\mathcal{O}}(\tau)\| \quad (3.19)$$

setting $R = 1$ from now on. Near $\tau = \pm\infty$, there will be finite corrections to the RHS of (3.19). Bring everything together, we find that

$$\begin{aligned} \text{LHS of Eq. (3.17)} &\lesssim \bar{\lambda}^2 \delta\tau^2 \exp(2c\Lambda^{2/3}) + \bar{\lambda} \delta\tau^2 \exp(c\Lambda^{2/3} + \ln \Lambda) + O(\delta\tau^3) \\ &= f \delta\tau^2 + O(\delta\tau^3) \end{aligned} \quad (3.20)$$

where $f = f(\bar{\lambda}, \Lambda)$ depends on the coupling λ and the UV cutoff Λ , but not on the size $\delta\tau$ of the interval. In (3.20) we have set $\tau \simeq 0$ for simplicity and omitted various constants. Since there are T timeslices in total, the total error made by discretizing is of the order of $T \cdot \delta\tau^2 \sim 1/T$, as we set out to prove.

We have been somewhat cavalier about the τ -dependence of the operator $\hat{\mathcal{O}}(\tau)$. This is justified away from the poles at $\tau = \pm\infty$, since the norm of both the operator $\hat{\mathcal{O}}(\tau)$ and its τ -derivative can be uniformly bounded on any compact interval. However, the Trotter formula can break down when wave functions blow up near the poles. More quantitatively, if $|\Psi\rangle$ is a given in-state, it may happen that the time-evolved state

$$U(\tau, -\infty)|\Psi\rangle = |\Psi\rangle - \bar{\lambda} \int_{-\infty}^{\tau} \frac{d\tau'}{(\cosh \tau')^d} \hat{\mathcal{O}}(\tau')|\Psi\rangle + \dots \quad (3.21)$$

fails to be normalizable, reflecting a physical UV divergence. For the matrix elements studied in this work, such divergences do not occur.

3.4 Other observables

The above derivation extends to correlation functions in a straightforward way. Suppose that we want to compute the one-point function of a scalar operator \mathcal{O}' :

$$\langle \mathcal{O}'(\tau, \mathbf{n}) \rangle_{\text{disc}} = \frac{1}{Z(0)} \int [d\phi] \mathcal{O}'(\tau, \mathbf{n}) e^{-S_0 - \delta S}. \quad (3.22)$$

We use the notation \mathcal{O}' to make clear that this operator is unrelated to the operator \mathcal{O} appearing in the action. Following the same steps as above, we find that

$$\langle \mathcal{O}'(\tau, \mathbf{n}) \rangle_{\text{disc}} = \langle \emptyset | U(\infty, \tau) \mathcal{O}'(\tau, \mathbf{n}) U(\tau, -\infty) | \emptyset \rangle. \quad (3.23)$$

In this normalization $\langle \mathbf{1} \rangle_{\text{disc}} = Z(\lambda)/Z(0) \neq 1$; it is therefore more natural to measure connected correlation functions:

$$\langle \mathcal{O}'(\tau, \mathbf{n}) \rangle_{\text{conn}} = \frac{Z(0)}{Z(\lambda)} \langle \mathcal{O}'(\tau, \mathbf{n}) \rangle_{\text{disc}} = \frac{\langle \emptyset | U(\infty, \tau) \mathcal{O}'(\tau, \mathbf{n}) U(\tau, -\infty) | \emptyset \rangle}{\langle \emptyset | U(\infty, -\infty) | \emptyset \rangle}. \quad (3.24)$$

In Eqs. (3.23) and (3.24) we can take the limit $\tau \rightarrow \mp\infty$, which corresponds to inserting \mathcal{O}' at the South (resp. North) pole:

$$\lim_{\tau \rightarrow -\infty} \langle \emptyset | U(\infty, \tau) \mathcal{O}'(\tau, \mathbf{n}) U(\tau, -\infty) | \emptyset \rangle = \langle \emptyset | U(\infty, -\infty) | \mathcal{O}' \rangle, \quad |\mathcal{O}'\rangle := \lim_{\tau \rightarrow -\infty} \mathcal{O}'(\tau, \mathbf{n}) | \emptyset \rangle. \quad (3.25)$$

Provided that \mathcal{O}' is normal-ordered, it is easy to show that the in-state $|\mathcal{O}'\rangle$ has finite norm and is independent of \mathbf{n} . The limit $\tau \rightarrow \infty$ can be treated similarly.

We can similarly consider higher-point functions. In general, measuring higher-point functions requires intermediate states that are not $\text{SO}(d)$ scalars. This is technically rather challenging in the framework described in this paper — see Sec. 5.1. However, we can measure antipodal two-point functions of ϕ . With an antipodal two-point function, we mean a correlator such as (2.6) measured at $\mathcal{S} = 1$. One way to compute such correlators is to insert the operators ϕ at both poles:

$$\langle \phi(\mathbf{N}) \phi(\mathbf{S}) \rangle_{\text{disc}} = \langle \phi(\mathbf{N}) | U(\infty, -\infty) | \phi(\mathbf{S}) \rangle \quad (3.26)$$

where the in- and out-states are defined as in Eq. (3.25). The connected two-point function can be constructed as in (3.24).

3.5 Comparison to Ref. [1]

The approach we have described above is closely related to earlier work by Al. B. Zamolodchikov [1] (which appeared in a slightly different form as [47]). In Ref. [1], the author considered a $\Delta = -2/5$ perturbation of the two-dimensional Yang-Lee CFT on S^2 ; the interacting partition function in that theory was computed by numerically integrating a time-dependent Schrödinger equation. In a subsequent paper, Grinza and Magnoli [48] studied a $\Delta = 1/8$ perturbation of the $2d$ Ising model using the same technique. In this section, we will spell out the connection between these $2d$ CFT papers and our method. What follows is independent from the rest of this paper and can be skipped on a first reading.

In the discussion that follows, two simple facts about CFTs will be important. First, we use that any conformally invariant theory can be mapped from S^d to the cylinder $\mathbb{R} \times S^{d-1}$ by a Weyl transformation (see e.g. [49, 50]). Concretely, a (scalar) local operator \mathcal{O} on S^d maps to its counterpart \mathcal{O}_{cyl} on the cylinder as follows:

$$\mathcal{O}(\tau, \mathbf{n}) = (\cosh \tau)^\Delta \mathcal{O}_{\text{cyl}}(\tau, \mathbf{n}) \quad (3.27)$$

where Δ is the scaling dimension of \mathcal{O} . Second, we recall that time translations on the cylinder are generated by the CFT dilatation operator D :

$$\mathcal{O}_{\text{cyl}}(\tau, \mathbf{n}) = e^{D\tau} \mathcal{O}_{\text{cyl}}(0, \mathbf{n}) e^{-D\tau}. \quad (3.28)$$

Bringing Eqs. (3.27) and (3.28) together, we can write every individual factor in Eq. (3.10) as

$$\mathbb{1} - \frac{\bar{\lambda}\delta\tau}{(\cosh \tau_k)^d} \hat{\mathcal{O}}(\tau_k) = e^{D\tau_k} \left[\mathbb{1} - \frac{\bar{\lambda}\delta\tau}{(\cosh \tau_k)^{d-\Delta}} \hat{\mathcal{O}}_{\text{cyl}}(0) \right] e^{-D\tau_k}. \quad (3.29)$$

Consequently, we obtain

$$\langle \Omega | U(\tau_f, \tau_i) | \Omega \rangle = \lim_{T \rightarrow \infty} \langle \Omega | \prod_{k=0}^{T-1} \left\{ \mathbb{1} - \delta\tau \left[D + \frac{\bar{\lambda}}{(\cosh \tau_k)^{d-\Delta}} \hat{\mathcal{O}}_{\text{cyl}}(0) \right] \right\} | \Omega \rangle \quad (3.30)$$

where $|\Omega\rangle$ is the radial quantization ground state, obeying $D|\Omega\rangle = 0$. In obtaining this formula, we use that

$$e^{-D\tau_k} e^{D\tau_{k-1}} = \mathbb{1} - \delta\tau D + O(\delta\tau^2).$$

Finally, if we define

$$|\psi(\tau)\rangle := U(\tau, -\infty) |\Omega\rangle \quad (3.31)$$

then Eq. (3.30) implies that $|\psi(\tau)\rangle$ satisfies the following Schrödinger equation:

$$-\frac{d}{d\tau} |\psi(\tau)\rangle = \left[D + \frac{\bar{\lambda}}{(\cosh \tau)^{d-\Delta}} \hat{\mathcal{O}}_{\text{cyl}}(0) \right] |\psi(\tau)\rangle \quad (3.32)$$

and the interacting partition function is recovered as the limit $Z(\lambda)/Z_{\text{CFT}} = \lim_{\tau \rightarrow \infty} \langle \Omega | \psi(\tau) \rangle$. After setting $d = 2$ this is essentially formula Eq. (5.9) from Ref. [1].⁷ An important feature of (3.30) is that the time coordinate τ only features via the kinematical factor $1/(\cosh \tau)^{d-\Delta}$: the perturbation $\hat{\mathcal{O}}_{\text{cyl}}(0)$ is a time-independent matrix. Moreover, the matrix elements of $\hat{\mathcal{O}}_{\text{cyl}}$ can be expressed as OPE coefficients of the UV CFT in question.

4 Cutoff effects

So far, we proposed a method to compute the partition function and correlation functions of scalar QFTs on S^d . Crucially, we truncated the Fock space to a finite-dimensional subspace characterized by a hard cutoff Λ . Since generic QFTs have UV divergences, additional Λ -dependent counterterms must be added to the action to regulate the theory in the UV.⁸ Moreover, in numerical computations it is not possible to send $\Lambda \rightarrow \infty$, and working at finite Λ induces a systematic error (similar to working at finite lattice spacing). Adding counterterms that vanish as $\Lambda \rightarrow \infty$ can reduce such systematic errors, cf. Symanzik's RG-improved lattice actions [51]. In the following sections, we will analyze the cutoff dependence of Z and of the antipodal two-point function for the ϕ^2 and ϕ^3 flows in perturbation theory and compute the relevant counterterms. We stress that the problem of reducing cutoff effects in Hamiltonian truncation is important and well-explored, see e.g. [27, Sec. VI] for a discussion of various methods. Recent work in this direction by various authors [29, 31–33, 36, 37] has culminated in extremely precise results for the ϕ^4 flow on $\mathbb{R} \times S^1$. Since there is no bona fide Hamiltonian on S^d , the approach we take is necessarily different from most of the literature, but will be similar in spirit to a perturbative method from Ref. [52].

⁷In that work the notation Δ refers to the eigenvalue of the L_0 generator of the Virasoro algebra, hence $\Delta_{\text{here}} = 2\Delta_{\text{there}}$.

⁸Since S^d is a compact manifold, there are no IR divergences.

4.1 Covariant results

In the next sections, we will compute observables using time-dependent perturbation theory in order to derive their cutoff dependence. Working in the continuum limit $\Lambda \rightarrow \infty$, the same observables may be computed using covariant methods. Here we briefly present the results of such a computation, performed using conformal perturbation theory in the case of the $m^2 = 0$ theory on S^3 . We have

$$\ln \frac{Z(\lambda_2, \lambda_3)}{Z(0, 0)} = \frac{\pi^2}{16} \bar{\lambda}_2^2 + \frac{1}{192(3-d)} \bar{\lambda}_3^2 + \dots \quad (4.1a)$$

$$R^{d-2} \langle \phi(N) \phi(S) \rangle_{\text{conn}} = \frac{1}{8\pi} - \frac{1}{4\pi} \bar{\lambda}_2 + \frac{\pi^2 - 4}{16\pi} \bar{\lambda}_2^2 + \frac{2\text{Catalan} - 1}{16\pi^2} \bar{\lambda}_3^2 + \dots \quad (4.1b)$$

$$R^{d-2} \langle \phi^2 \rangle_{\text{conn}} = -\frac{1}{8} \bar{\lambda}_2 + \frac{1}{8} \bar{\lambda}_2^2 + \frac{1}{16\pi^2} \bar{\lambda}_3^2 + \dots \quad (4.1c)$$

omitting terms of order λ_2^3 and λ_3^4 . The quantity **Catalan** denotes Catalan's constant, $\text{Catalan} \simeq 0.916$. The $1/(3-d)$ pole in the partition function reflects a logarithmic UV divergence that will be discussed later; all other terms in the perturbative expansion are finite.

4.2 Leading contribution to the partition function

In what follows, we turn to the computation of the partition function for a general perturbation of the form (3.1). The leading correction to $Z(\lambda)$ — cf. formula (3.6) — reads

$$\frac{Z(\lambda)}{Z(0)} = 1 + \bar{\lambda}^2 \int_{-\infty}^{\infty} \frac{d\tau_1}{(\cosh \tau_1)^d} \int_{-\infty}^{\tau_1} \frac{d\tau_2}{(\cosh \tau_2)^d} \langle \hat{\mathcal{O}}(\tau_1) \hat{\mathcal{O}}(\tau_2) \rangle_0 + O(\bar{\lambda}^3) \quad (4.2)$$

where $\hat{\mathcal{O}}(\tau)$ is the spatially integrated operator as defined in (3.2). We are assuming that \mathcal{O} is normal-ordered, such that $\langle \mathcal{O} \rangle_0$ vanishes. The two-point function $\langle \hat{\mathcal{O}}(\tau_1) \hat{\mathcal{O}}(\tau_2) \rangle_0$ does not have a universal form — it's not constrained by any symmetries. However, at short distances we can approximate the full $\langle \mathcal{O} \mathcal{O} \rangle_0$ correlator by

$$\langle \mathcal{O}(\tau_1, \mathbf{n}_1) \mathcal{O}(\tau_2, \mathbf{n}_2) \rangle_0 \underset{\mathcal{S} \rightarrow 0}{\sim} \frac{a}{(4R^2 \mathcal{S})^\Delta} = a \left(\frac{\cosh \tau_1 \cosh \tau_2}{2R^2} \right)^\Delta \frac{1}{(\cosh \tau_{12} - \mathbf{n}_1 \cdot \mathbf{n}_2)^\Delta} \quad (4.3)$$

for some constants $a > 0$ and Δ , writing $\tau_{12} \equiv \tau_1 - \tau_2$.⁹ In writing (4.3) only the most singular term as $\mathcal{S} \rightarrow 0$ is taken into account, and any subleading terms $\propto 1/\mathcal{S}^{\Delta'}$ with $\Delta' < \Delta$ are omitted. This approximation can be justified *a posteriori*. In the theory of the massive boson with $\mathcal{O} = \phi^n$, the coefficients Δ and a are given by

$$\Delta = n(\tfrac{1}{2}d - 1) \quad \text{and} \quad a = \frac{n!}{[(d-2)S_d]^n} \quad (4.4)$$

provided that $d > 2$. Notice that the coefficients Δ and a do not depend on the bare mass m^2 , although all subleading terms do. In $d = 2$ the approximation (4.3) breaks down, since at short distances the correlator $\langle \phi^n \phi^n \rangle$ scales as $(\ln \mathcal{S})^n$.¹⁰ Integrating over angles in (4.3), we obtain

$$\langle \hat{\mathcal{O}}(\tau_1) \hat{\mathcal{O}}(\tau_2) \rangle_0 \stackrel{\tau_1 \geq \tau_2}{=} a S_d^2 (\cosh \tau_1 \cosh \tau_2 e^{-\tau_{12}})^\Delta {}_2F_1 \left[\begin{matrix} \Delta, \Delta - d/2 + 1 \\ d/2 \end{matrix} \middle| e^{-2\tau_{12}} \right]. \quad (4.5)$$

⁹In passing, we remark that if the UV theory is a CFT and \mathcal{O} has a well-defined scaling dimension Δ , then formula (4.3) is exact. This can easily be checked by applying a Weyl transformation to (4.3). The choice $a = 1$ corresponds to a flat-space two-point function normalized as $\langle \mathcal{O}(x) \mathcal{O}(y) \rangle = |x - y|^{-2\Delta}$.

¹⁰It is perhaps possible to adapt the strategy of Refs. [31, 32, 36] to deal with such correlators.

Working at finite cutoff means that only certain intermediate states are allowed, i.e.

$$\langle \hat{\mathcal{O}}(\tau_1) \hat{\mathcal{O}}(\tau_2) \rangle_0 \longrightarrow \sum_{|\psi\rangle} \langle \emptyset | \hat{\mathcal{O}}(\tau_1) | \psi \rangle \langle \psi | \hat{\mathcal{O}}(\tau_2) | \emptyset \rangle, \quad E(|\psi\rangle) \leq \Lambda. \quad (4.6)$$

Eq. (4.5) does not refer to any explicit quantization. However, if we Taylor expand the hypergeometric function in (4.5), the k -th term corresponds roughly to an intermediate state of energy $E \sim (\Delta + 2k)/R$ (taking into account the $\exp(-\Delta\tau_{12})$ prefactor). Hence we can identify $\Lambda \sim (\Delta + 2k_{\max})/R$, at least for very large values of Λ . This leads to the following estimate for $Z(\lambda)$ at cutoff Λ :

$$\frac{Z(\lambda)}{Z(0)} = 1 + a\bar{\lambda}^2 \mathcal{B}(\Lambda) + \dots, \quad \text{where} \quad \mathcal{B}(\Lambda) = S_d^2 \sum_{k=0}^{\Lambda R/2} \frac{(\Delta)_k (\Delta - d/2 + 1)_k}{k! (d/2)_k} I_k \quad (4.7)$$

and $I_k = I_k(\Delta, d)$ is the following definite integral:

$$I_k := \int_{-\infty}^{\infty} \frac{d\tau_1}{(\cosh \tau_1)^{d-\Delta}} \int_{-\infty}^{\tau_1} \frac{d\tau_2}{(\cosh \tau_2)^{d-\Delta}} e^{-(\Delta+2k)\tau_{12}}. \quad (4.8)$$

The integrals (4.8) are convergent and can be evaluated in closed form, if desired. However, we're interested in the tail of the sum in (4.7), and therefore we only need the large- k asymptotics of I_k :

$$I_k \stackrel{k \gg 1}{\sim} \frac{B(d - \Delta, \frac{1}{2})}{d + 2k} + O(1/k^2) \quad (4.9)$$

where $B(x, y)$ is the Euler beta function — this is a special case of Eq. (B.6).

We are now ready to determine the cutoff dependence of the sum (4.7). Using the asymptotics (4.9), we find that the summand in (4.7) scales as $k^{2\Delta-d-1}$. This means that for $\Delta < d/2$ the partition function is finite, whereas for $\Delta \geq d/2$ it is divergent. The case $\Delta > d/2$ will not be important in the present work. Treating the cases $\Delta < d/2$ and $\Delta = d/2$ separately, we obtain

$$\Delta < d/2: \quad \mathcal{B}(\Lambda) = 2^{d-2\Delta-2} S_{d+1} S_d B(\tfrac{1}{2}d - \Delta, \tfrac{1}{2}d) - \frac{\nu(\Delta)}{(\Lambda R)^{d-2\Delta}} + O(1/\Lambda^{d-2\Delta+1}), \quad (4.10a)$$

$$\nu(\Delta) = \frac{2^{d-2\Delta-2} S_d^2 \Gamma(\tfrac{1}{2}d) B(d - \Delta, \tfrac{1}{2})}{(\tfrac{1}{2}d - \Delta) \Gamma(\Delta) \Gamma(\Delta - \tfrac{1}{2}d + 1)}$$

$$\Delta = d/2: \quad \Lambda \frac{d}{d\Lambda} \mathcal{B}(\Lambda) = \frac{(2\pi)^d}{\Gamma(d)} + O(1/\Lambda). \quad (4.10b)$$

In the finite case ($\Delta < d/2$) we can compensate for the leading truncation error by shifting the Casimir energy as follows:

$$\Delta < d/2: \quad S \mapsto S - a \frac{\nu(\Delta)}{S_{d+1}} \frac{\lambda^2}{\Lambda^{d-2\Delta}} \int_{S^d} \sqrt{g} d^d x. \quad (4.11a)$$

If $\Delta = d/2$, a logarithmic counterterm must be added in order to make the partition function well-defined:

$$\Delta = d/2: \quad S \mapsto S + a(S_d/2) \lambda^2 \ln(\Lambda/\mu) \int_{S^d} \sqrt{g} d^d x \quad (4.11b)$$

where μ is an arbitrary energy scale. The only other dimensionful quantity (other than R) is λ , hence we can take $\mu = |\lambda|^{2/d}$ for definiteness. However, changing μ merely shifts the Casimir energy density by an amount proportional to λ^2 .

Notice that both counterterms in (4.11) are completely local. In general, it is not true that only local counterterms are generated in our scheme. For instance, if we attempt to further RG-improve

the action, we will encounter terms that explicitly depend on the radius R . For instance, subleading terms in (4.10a) are of the form $1/(\Lambda R)^{d-2\Delta+n}$, and only for even n such a term can be compensated by adding a local counterterm to the action. Non-local counterterms are a generic feature of hard energy cutoffs, and they are discussed in more detail e.g. in Refs. [29, 32, 36, 40] in different settings.

Interactions with $\Delta > d/2$ can be addressed in a similar fashion. For instance, in the $3d$ ϕ^4 theory, a linearly divergent counterterm must be added, similar to the logarithmically divergent counterterm from Eq. (4.11b).

4.3 LO computation for ϕ^2 and ϕ^3 interactions

In the previous section, we provided a rough estimate of the cutoff dependence of the partition function, based on a general argument that did not refer to a specific action. Next, we will consider the ϕ^2 and ϕ^3 interactions on S^d in the Hamiltonian picture of Sec. 3 and compute the cutoff dependence of Z using time-dependent perturbation theory. The fact that both approaches agree provides a useful consistency check.

To leading order, the partition function Z for a cubic theory with Lagrangian (1.2) is given by

$$\ln \frac{Z(\lambda_2, \lambda_3)}{Z(0, 0)} = \bar{\lambda}_2^2 \mathcal{C}_2(\Lambda) + \bar{\lambda}_3^2 \mathcal{C}_3(\Lambda) + O(\lambda_2^3, \lambda_3^4) \quad (4.12)$$

The diagrams $\mathcal{C}_n(\Lambda)$ are given by

$$\mathcal{C}_n(\Lambda) = \frac{1}{n!} \sum_{\{\ell_i\}} \Theta(\varepsilon(\ell_1) + \dots + \varepsilon(\ell_n) \leq \Lambda) A_n(\ell_1, \dots, \ell_n) Q(\ell_1, \dots, \ell_n) \quad (4.13)$$

where

$$A_n(\ell_1, \dots, \ell_n) := \int_{S^{d-1}} d\mathbf{n}_1 d\mathbf{n}_2 \prod_{i=1}^n \frac{n_{\ell_i}^d}{S_d} C_{\ell_i}^d(\mathbf{n}_1 \cdot \mathbf{n}_2) \quad (4.14)$$

and

$$Q(\ell_1, \dots, \ell_n) := \int_{\mathbb{R}} \frac{d\tau}{(\cosh \tau)^d} \int_{-\infty}^{\tau} \frac{d\tau'}{(\cosh \tau')^d} \prod_{i=1}^n K_{\ell_i}(\tau) K_{\ell_i}(-\tau'). \quad (4.15)$$

The sum in (4.13) runs over all unordered tuples $\{\ell_1, \dots, \ell_n\}$, but the Θ function only selects intermediate states with energy $E \leq \Lambda$. The integrals A_n can be performed analytically for all n and d ; closed-form expressions for $n = 2, 3$ are stated in Sec. A. On the other hand, the $Q(\ell_i)$ integrals are rather complicated, at least for general values of m^2 and d , and as such must be computed numerically.

Let us first consider $n = 2$ in three dimensions. In this case we know that $\mathcal{C}_2(\Lambda)$ has a finite limit as $\Lambda \rightarrow \infty$. For definiteness, let's consider the massless case, for which the function $\mathcal{C}_2(\Lambda)$ can be computed analytically. To wit

$$\begin{aligned} \mathcal{C}_2(\Lambda) \Big|_{m^2=0, d=3} &= \sum_{\ell=0}^{\infty} \Theta(2\varepsilon(\ell) \leq \Lambda) (\ell + \tfrac{1}{2}) Q(\ell, \ell), \\ Q(\ell, \ell) \Big|_{m^2=0, d=3} &= \frac{2}{(2\ell+1)^2} \left[{}_3F_2 \left(\begin{matrix} 1, 1, 1 \\ 3, \ell + \frac{3}{2} \end{matrix} \middle| 1 \right) - 1 \right] \underset{\ell \rightarrow \infty}{\sim} \frac{1}{6\ell^3}. \end{aligned} \quad (4.16)$$

In obtaining this result we make use of the integral $G_1(\alpha, \beta)$ from Eq. (B.5b). Using the above asymptotics, it can be shown that

$$\mathcal{C}_2(\Lambda) \underset{\Lambda \rightarrow \infty}{\sim} \frac{\pi^2}{16} - \frac{1}{3\Lambda R} + O(1/\Lambda^2). \quad (4.17)$$

According to Eq. (4.11a), the leading $1/\Lambda$ truncation error in (4.17) can be compensated for by adding the following counterterm:

$$\delta S = -\frac{1}{6\pi^2} \frac{\lambda_2^2}{\Lambda} \int_{S^3} \sqrt{g} d^3x = -\frac{1}{3\Lambda R} \bar{\lambda}_2^2. \quad (4.18)$$

Comparing Eqs. (4.17) and (4.18), we find a perfect agreement between the general argument from the previous section and the specific computation in Eq. (4.16).

We can treat the cubic ($n = 3$) interaction in a similar fashion. Now, we have to consider the behavior of

$$\mathcal{C}_3(\Lambda) = \frac{1}{6} \sum_{\ell_1 \ell_2 \ell_3} \Theta(\varepsilon(\ell_1) + \varepsilon(\ell_2) + \varepsilon(\ell_3) \leq \Lambda) A_3(\ell_1, \ell_2, \ell_3) Q(\ell_1, \ell_2, \ell_3) \quad (4.19)$$

at large Λ . The coefficient A_3 is computed in Eq. (A.10), and in the massless limit we furthermore have

$$Q(\ell_i) \Big|_{m^2=0, d=3} = \frac{2\pi}{(2\ell_1+1)(2\ell_2+1)(2\ell_3+1)} \left[\pi \frac{\left(\frac{3}{2}\right)_L^2}{L!^2} - (4L+3) \right], \quad L = \frac{1}{2}(\ell_1 + \ell_2 + \ell_3). \quad (4.20)$$

A precise determination of (4.19) is somewhat difficult. However, it is easy to argue that $\mathcal{C}_3(\Lambda)$ diverges logarithmically in $d = 3$, as was already predicted in Eq. (4.1a). To prove this, consider the variation $\partial \mathcal{C}_3 / \partial \Lambda$ at large Λ , such that the ℓ_i can be treated as continuous variables. The sum over the ℓ_i becomes an integral that localizes on a two-simplex $\ell_1 + \ell_2 + \ell_3 \simeq \Lambda R$ of volume $\sim (\Lambda R)^2$. Using the explicit formula for A_3 , we have $A_3(\ell_i) \sim \Lambda R$ on this simplex. Moreover, from (4.20) it follows that $Q(\ell_i) \sim 1/(\Lambda R)^4$. Consequently,

$$d = 3 : \quad \frac{\partial \mathcal{C}_3(\Lambda)}{\partial \Lambda} \Big|_{\Lambda \rightarrow \infty} \sim (\Lambda R)^2 \cdot (\Lambda R) \cdot (\Lambda R)^{-4} = 1/(\Lambda R) \quad (4.21)$$

up to a multiplicative constant that we have not attempted to compute. Following the discussion from the previous section, this logarithmic divergence was to be expected as well, since in $d = 3$ we have $\Delta_{\phi^3} = 3/2 = d/2$. According to Eq. (4.11b), the theory can be made UV-finite by adding the following counterterm

$$\delta S = \frac{1}{192\pi^2} \ln(\Lambda/|\lambda_3|^{2/3}) \lambda_3^2 \int_{S^3} \sqrt{g} d^3x = \frac{\bar{\lambda}_3^2}{96} \ln(\Lambda/|\lambda_3|^{2/3}) \quad (4.22)$$

which renormalizes \mathcal{C}_3 . Consequently the subtracted quantity

$$\mathcal{C}_3^{\text{ren}}(\Lambda) := \mathcal{C}_3(\Lambda) - \frac{1}{96} \ln(\Lambda/|\lambda_3|^{2/3}) \quad (4.23)$$

should have a finite limit as $\Lambda \rightarrow \infty$, as we have checked numerically up to large cutoffs ($\Lambda R \sim 100$).

Both in the case of the \mathcal{C}_2 and \mathcal{C}_3 diagrams in $d = 3$, we estimated truncation errors up to those of order $1/\Lambda$ resp. $\ln \Lambda$. In principle, it is possible to compute further RG-improvement counterterms by analyzing terms of order $1/\Lambda^2$ resp. $1/\Lambda$. Unlike the leading counterterms (4.18) and (4.22), all subleading counterterms will depend on the bare mass m^2 . In order to compute such subleading counterterms in general, higher-order diagrams in perturbation theory must be taken into account as well.

4.4 Antipodal correlation function at (N)LO

In the previous section, we considered the cutoff dependence of the partition function Z . Here we will turn our attention to the antipodal correlation function $\langle \phi(N) \phi(S) \rangle_{\text{conn}}$, using it to fix an additional counterterm. Working at finite cutoff Λ , we have

$$R^{d-2} \langle \phi(N) \phi(S) \rangle_{\text{disc}} = R^{d-2} G(\mathcal{S} = 1) + \bar{\lambda}_2^2 \mathcal{D}_{2,1}(\Lambda) + \bar{\lambda}_2^2 \mathcal{D}_{2,2}(\Lambda) + \bar{\lambda}_3^2 \mathcal{D}_{3,2}(\Lambda) + \dots \quad (4.24)$$

omitting higher-order diagrams and disconnected diagrams. The free contribution

$$G(\mathcal{S} = 1) = \frac{\kappa^2}{S_d R^{d-2}}, \quad \kappa \equiv \lim_{\tau \rightarrow \infty} K_0(\tau), \quad (4.25)$$

does not depend on the cutoff scale Λ .¹¹ The same applies to the leading-order contribution $\mathcal{D}_{2,1}$, since

$$\mathcal{D}_{2,1}(\Lambda) = -\frac{\kappa^2}{S_d} \int_{\mathbb{R}} \frac{d\tau}{(\cosh \tau)^d} K_0(-\tau) K_0(\tau). \quad (4.26)$$

Surprisingly, the next-to-leading term $\mathcal{D}_{2,2}$ is cutoff-insensitive as well. There are two different diagrams contributing to this quantity, yielding

$$\mathcal{D}_{2,2}(\Lambda) = \frac{\kappa^2}{S_d} \int_{\mathbb{R}} \frac{d\tau}{(\cosh \tau)^d} \int_{-\infty}^{\tau} \frac{d\tau'}{(\cosh \tau')^d} [K_0(-\tau) K_0(\tau) K_0(-\tau') K_0(\tau') + K_0(\tau)^2 K_0(-\tau')^2]. \quad (4.27)$$

In all of the above cases, only intermediate states of energy $E = \varepsilon(0)$ or $E = 3\varepsilon(0)$ are propagated.

Finally, consider the leading contribution generated by the ϕ^3 term. There are infinitely many intermediate states contributing, indexed by a spin ℓ , and only spins up to $\ell_{\max} \sim \Lambda R/2$ are below the cutoff and contribute. Explicitly, we have

$$\begin{aligned} \mathcal{D}_{3,2}(\Lambda) = \frac{1}{2} \frac{\kappa^2}{S_d^2} \sum_{\ell=0}^{\infty} n_{\ell}^d \int_{\mathbb{R}} \frac{d\tau}{(\cosh \tau)^d} \int_{-\infty}^{\tau} \frac{d\tau'}{(\cosh \tau')^d} K_{\ell}(\tau)^2 K_{\ell}(-\tau')^2 \\ \times [\Theta(2\varepsilon(\ell) \leq \Lambda) K_0(-\tau) K_0(\tau') + \Theta(2\varepsilon(\ell) + 2\varepsilon(0) \leq \Lambda) K_0(\tau) K_0(-\tau')]. \end{aligned} \quad (4.28)$$

The two terms in (4.28) correspond to diagrams with different time-orderings. In the massless limit the sum (4.28) can be computed in closed form using the integral (B.5b). Setting $d \rightarrow 3$ this yields

$$\begin{aligned} \mathcal{D}_{3,2}(\Lambda) \Big|_{m^2=0, d=3} = \frac{1}{32\pi} \sum_{\ell} \frac{\Theta(2\varepsilon(\ell) \leq \Lambda)}{2\ell+1} \left[\frac{4}{\pi} \frac{\ell!^2}{(\frac{1}{2})_{\ell}^2} - 4\ell - 1 \right] \\ + \frac{\Theta(2\varepsilon(\ell) + 2\varepsilon(0) \leq \Lambda)}{2\ell+1} \left[\pi \frac{(\frac{3}{2})_{\ell}^2}{\ell!^2} - 4\ell - 3 \right]. \end{aligned} \quad (4.29)$$

Evaluating (4.29) in the limit of large Λ , we find

$$(\dots) = \frac{2\text{Catalan} - 1}{16\pi^2} - \frac{1}{128\pi\Lambda R} + O(1/\Lambda^2) \quad (4.30)$$

consistent with (4.1b). We would like to compensate for this $1/\Lambda$ truncation error by adding a (local) counterterm proportional to ϕ^2 :

$$\delta S = -c_3 \frac{\lambda_3^2}{\Lambda} \int_{S^3} \sqrt{g} d^d x \phi^2(x) \quad (4.31)$$

where c_3 is a dimensionless constant. The counterterm (4.31) shifts the $\langle \phi(N) \phi(S) \rangle$ two-point function by an amount

$$\delta \langle \phi(N) \phi(S) \rangle = \frac{c_3}{2\pi} \frac{\bar{\lambda}_3^2}{\Lambda R^2} + O(1/\Lambda^2). \quad (4.32)$$

By comparing with (4.30), we conclude that setting $c_3 = 1/64$ eliminates the leading cutoff error completely.

¹¹This is a consequence of the North-South kinematics of the correlator in question: for a general two-point function $\langle \phi(\tau_1) \phi(\tau_2) \rangle$, an infinite tower of intermediate states of the form $a_{\ell j}^{\dagger} |\emptyset\rangle$ contributes to the Green's function (2.15). Yet in the limit where either $\tau_1 \rightarrow \infty$ or $\tau_2 \rightarrow -\infty$, only the state with $\ell = j = 0$ contributes (since all other K_{ℓ} vanish).

Ultimately, we are interested in computing the *connected* antipodal two-point function. So far we have been cavalier about disconnected contributions to the $\langle \phi(N)\phi(S) \rangle$ correlator in Eq. (4.24). At order λ_3^2 , we have discarded one disconnected diagram. Had we used a fully local regulator, then this disconnected diagram would cancel after dividing by the partition function $Z(\lambda_3)/Z(0)$. Unfortunately, in our hard-cutoff scheme the contribution of the two diagrams does not cancel entirely. There is a spurious contribution $\tilde{\mathcal{D}}$ to the antipodal correlation function at order λ_3^2 :

$$R^{d-2} \langle \phi(N)\phi(S) \rangle_{\text{conn}} = (\text{connected diagrams}) + \bar{\lambda}_3^2 \tilde{\mathcal{D}}(\Lambda) + O(\lambda_3^4),$$

$$\tilde{\mathcal{D}}(\Lambda) = -\frac{\kappa^2}{6S_d} \sum_{\{\ell_i\}} \Theta(\Lambda - 2\varepsilon(0) \leq \varepsilon(\ell_1) + \varepsilon(\ell_2) + \varepsilon(\ell_3) < \Lambda) A_3(\ell_1, \ell_2, \ell_3) Q(\ell_1, \ell_2, \ell_3). \quad (4.33)$$

In order to reproduce the correct continuum limit (4.1b), it is crucial that $\tilde{\mathcal{D}}(\Lambda)$ vanishes as $\Lambda \rightarrow \infty$. This is not immediately obvious. By comparing the summand of (4.33) to Eq. (4.13), it is however easy to see that

$$\tilde{\mathcal{D}}(\Lambda) = -\varepsilon(0) \frac{2\kappa^2}{S_d} \frac{\partial \mathcal{C}_3(\Lambda)}{\partial \Lambda} \quad (4.34)$$

up to errors that can be neglected when $\Lambda \gg \varepsilon(0)$. Since in $d = 3$ the function \mathcal{C}_3 grows logarithmically with Λ , we conclude that $\tilde{\mathcal{D}}(\Lambda)$ vanishes as $1/\Lambda$ as the cutoff is removed, as desired.

5 Nonperturbative results

In the first half of this paper, a method to compute observables on S^d was proposed for scalar QFTs on the d -sphere, and subsequently the leading counterterms generated by ϕ^2 and ϕ^3 interactions were computed. In what follows, we will test our method numerically, i.e. in the strong coupling regime. First, we explain in more detail how the computation in question is performed. Second, we turn to the ϕ^2 interaction on S^3 , where our numerical data can be compared to analytic formulas. Finally, we consider the $i\phi^3$ interaction, where we will check that the counterterm prescription from Sec. 4 renders the theory UV-finite.

5.1 Implementation

The framework used to perform nonperturbative computations in our scheme has been explained in Secs. 3.1 and 3.2. Here, we will provide additional details that are needed to reproduce our results. Some non-essential comments are discussed in Appendix C. Suppose that the spacetime dimension d , the bare mass m^2 and the cutoff Λ are fixed. Then any computation proceeds in three steps, schematically:

1. Generate a basis of all Fock space states $|\psi_i\rangle$ with energy $E(|\psi_i\rangle)$ below the cutoff Λ ;
2. Generate matrices $V_n(\tau) \equiv [V_n(\tau)]_i^j$ defined as

$$R^{n(d/2-1)} \int_{S^{d-1}} d\mathbf{n} \phi^n(\tau, \mathbf{n}) |\psi_i\rangle =: \sum_j [V_n(\tau)]_i^j |\psi_j\rangle + \text{states above the cutoff};$$

3. Compute observables using the Trotter formula (3.10).

Let us provide some additional details regarding these three steps. Concerning the first step, the reader will remark that the total number of Fock space states grows rapidly (exponentially) with the

cutoff Λ . Listing *all* Fock space states below the cutoff Λ , it would be prohibitive to store the matrices $V_n(\tau)$ in memory if $\Lambda R \gtrsim 15$. However, the Dyson operator U is invariant under $O(d)$ transformations acting on the spherical coordinate \mathbf{n} , i.e. both under $SO(d)$ transformations and a parity transformation (if d is odd, parity acts as $\mathbf{n} \rightarrow -\mathbf{n}$). In the case of the partition function (3.8) and the antipodal two-point function (3.26), all in- and out-states are $O(d)$ scalar states. Consequently, only $O(d)$ scalar intermediate states are needed, which strongly constrains the list of states $|\psi_i\rangle$ that must be taken into account.

Let's specialize to $d = 3$, denoting the generators of $SO(3)$ as L_\pm and L_z . It is easy to generate a basis of parity-even states obeying $L_z|\psi\rangle = 0$, and it tedious but straightforward to select all states that in addition obey $L_\pm|\psi\rangle = 0$. For various values of Λ , a counting of the dimension of the Fock space $\mathcal{F}(\Lambda)$ for $d = 3$ and $m^2 = 0$ is shown in Table 1. (If $\lambda_3 = 0$, the action is invariant under a \mathbb{Z}_2 global symmetry $\phi \rightarrow -\phi$ which further constrains the Fock space.)

ΛR	all states	$L_z = 0$ & parity-even	scalars
10	6057	422	58
15	193155	9231	439
20	4425606	166802	3782

Table 1: Counting the number of Fock space states obeying $O(d)$ selection rules in $d = 3$ for $m^2 = 0$, for various values of the cutoff Λ .

The second step, i.e. the computation of the matrices $V_n(\tau)$, is again tedious but straightforward. The normal-ordered operators ϕ^2 and ϕ^3 are defined explicitly in Eq. (2.16). Consequently, the action of either of these operators on a Fock space state $|\psi_i\rangle$ is completely determined by the canonical commutation relations. Note that the matrix elements $[V_n(\tau)]_i^j$ depend on τ only through the functions $K_\ell(\tau)$ and $K_\ell(-\tau)$.

The computation of observables using the Trotter formula is straightforward. Consider for instance the partition function (3.8), given couplings λ_n and a number of timeslices T . We can directly use formula (3.10) to compute an estimate for $Z(\lambda_n)/Z(0)$. In pseudocode, our algorithm reads:

```

 $|\psi\rangle \leftarrow |\emptyset\rangle$ 
for  $k = 0, \dots, T - 1$  :
     $z \leftarrow (k + \frac{1}{2})/T$ 
     $|\psi\rangle \leftarrow |\psi\rangle - \frac{S_{d+1}}{S_d T} \sum_n \frac{\bar{\lambda}_n}{n!} V_n(\tau(z)) |\psi\rangle$ 
out  $\leftarrow \langle \emptyset | \psi \rangle$ .

```

If counterterms are added to the action, the fourth line needs to be modified in an obvious way. With $|\psi\rangle$ we denote an N -dimensional vector, where N is the number of scalar Fock space states. Above we have used the z -coordinate introduced in Eq. (3.16), as well as the Jacobian

$$\frac{\delta\tau}{(\cosh \tau)^d} = \frac{1}{z'(\tau)} \frac{\delta z}{(\cosh \tau(z))^d} = \frac{S_{d+1}}{S_d} \delta z.$$

Since times are uniformly sampled in z , it follows that $\delta z = 1/T$.

We have performed all of these steps in **Mathematica** on a laptop computer. The only subtlety in implementing the above algorithm has to do with numerical precision. The algorithm in question performs a huge number of floating point operations (addition and multiplication). Given a truncated

Fock space of dimension N and T timeslices, an estimate of the number of floating point operations is $N_{\text{op}} = N^2 T$, which for $\Lambda R = 20$ and $T = 2500$ evaluates to $N_{\text{op}} \sim 4 \cdot 10^{10}$. Consequently, using `MachinePrecision` does not always yield satisfactory results, and typically it is necessary to work with arbitrary-precision numbers. The number of digits required depends on T , Λ and the couplings $\bar{\lambda}_n$; in this work we have used up to 300 digits (out of an abundance of caution).

Finally, let us make a remark about the discretization of the Trotter formula, i.e. the number T of timeslices that is used. In practice, we repeat the same computation of an observable f for a range of values T up to some T_{max} , labeling the data points as $f(T)$. Next, we verify that the $1/T$ falloff of the discretization error is satisfied, which allows for an extrapolation to $T = \infty$. This procedure yields an estimate of the observable $f(T)$ as $T \rightarrow \infty$ together with an error estimate $\delta f_{\text{disc}} = |f(\infty) - f(T_{\text{max}})|$.

5.2 ϕ^2 flow on S^3

Let us first consider the case where we only turn on a ϕ^2 interaction on S^3 with coupling λ_2 . This is nothing but the Gaussian action of a boson with a physical mass $M^2 = m^2 + \lambda_2$. The partition function on S^d can be computed exactly, yielding:¹²

$$\ln \frac{Z(M)}{Z(m)} = \frac{1}{2} \int_{m^2 R^2}^{M^2 R^2} dx [q(x) - q(m^2 R^2)] \quad \text{where} \quad q(x) = \frac{\pi}{2} \frac{\sqrt{\frac{1}{4} - x}}{\tan \pi \sqrt{\frac{1}{4} - x}}. \quad (5.1)$$

Likewise, the antipodal two-point function $\langle \phi(N)\phi(S) \rangle_{\text{conn}}$ correlator can be obtained from the Green's function (2.10), namely

$$\langle \phi(N)\phi(S) \rangle_{\text{conn}} = \frac{1}{4\pi^2 R} \Gamma(1 + \sqrt{\frac{1}{4} - M^2 R^2}) \Gamma(1 - \sqrt{\frac{1}{4} - M^2 R^2}) \underset{R \rightarrow \infty}{\sim} \frac{M}{2\pi} \exp(-\pi M R). \quad (5.2)$$

The large- R behavior of (5.2) simply shows that the correlation length of the massive boson equals $\xi = 1/M$, since the geodesic distance between the two poles equals πR .

We will compare the exact predictions (5.1) and (5.2) to numerical data obtained using our scheme, setting $m^2 = 0$ from now on. After adding the RG improvement term (4.18), the action reads

$$S = S_0 + \int_{S^3} \sqrt{g} d^3 x \left[\frac{1}{2} M^2 \phi^2(x) - \frac{M^4}{6\pi^2 \Lambda} \right]. \quad (5.3)$$

We will use values of $T \leq T_{\text{max}} = 2500$ and $\Lambda R \leq 20$, scanning over couplings up to $M^2 R^2 = 10$. For a given coupling $M^2 R^2$, we expect and observe a truncation error that decreases as $1/\Lambda^2$. Consequently, we can extrapolate the numerical data to $\Lambda = \infty$, assigning error bars based on this extrapolation. In Fig. 2 (left), we plot our numerical results and compare them to Eq. (5.1). For all radii R in this range we find agreement within error bars, with relative errors at the % level or better. This is an excellent consistency check of our method, because the theory is strongly coupled in this regime. To make this precise, the observable $\ln Z(M)$ admits an asymptotic perturbative expansion $\sum_n \alpha_n (M^2 R^2)^n$ with coefficients α_n that are sign-alternating and that grow exponentially with n . Therefore perturbation theory is a poor approximation to the exact result unless $M^2 R^2 \ll 1$.

¹²A simple way to obtain (5.1) is through the identity

$$\frac{d}{d\lambda} \ln \frac{Z(\lambda)}{Z(0)} = -S_{d+1} R^d \langle \mathcal{O} \rangle_{\text{conn}, \lambda}$$

which holds for a general perturbation of the form (3.1). In the case at hand, $\langle \mathcal{O} \rangle = \langle \phi^2 \rangle$ can be extracted from the short-distance behaviour of the Green's function (2.10).

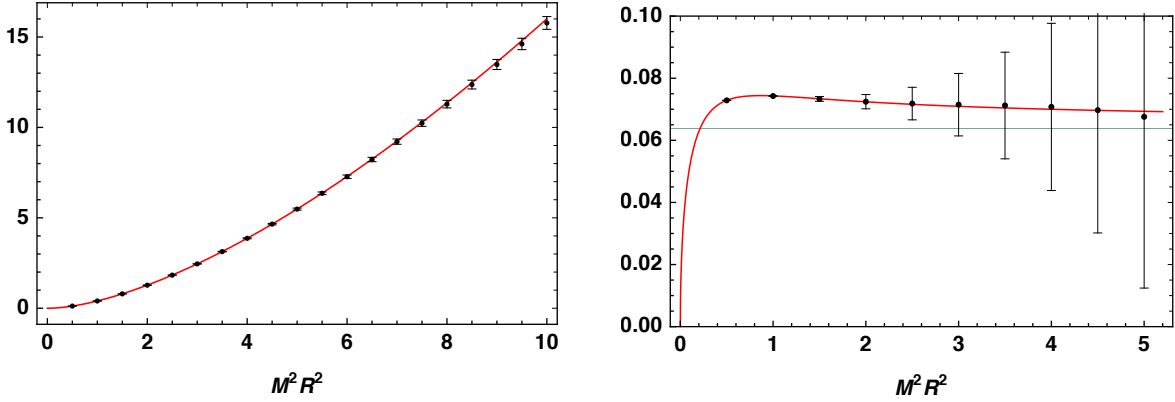


Figure 2: **Left:** the log of the partition function, $\ln Z(M)/Z(0)$, for the $\frac{1}{2}M^2\phi^2$ flow (5.3), scanning over a range of values of $M^2 R^2$ (horizontal axis). Black dots with error bars: numerical data; **red** curve: exact result. **Right:** the same observable, recomputed using the renormalized action S_{ren} from Eq. (5.4). **Green** horizontal line: F_{scalar} , the $M^2 R^2 \rightarrow \infty$ limit of the free energy.

The ϕ^2 theory flows from the free boson CFT in the UV to a gapped (empty) QFT in the IR. After adding two curvature counterterms from Eq. (1.1), we expect that the free energy in the limit $MR \rightarrow \infty$ asymptotes to the F -coefficient of the free scalar CFT, since the empty QFT has $F = 0$. The necessary counterterms can be extracted from formula (5.1) — see for instance the discussion in Appendix A.1 of [9]. Consequently, if we recompute $Z(M)$ using the renormalized action¹³

$$S_{\text{ren}} = S + \int_{S^3} \sqrt{g} d^3x \left[\frac{M^3}{12\pi} - \frac{M}{192\pi} \mathcal{R} \right] \quad (5.4)$$

we expect that

$$\ln \frac{Z(M)}{Z(0)} \underset{R \rightarrow \infty}{\sim} F_{\text{scalar}} + O(1/MR), \quad F_{\text{scalar}} = \frac{\ln 2}{8} - \frac{3\zeta(3)}{(4\pi)^2} \simeq 0.0638. \quad (5.5)$$

The value of F_{scalar} is usually derived using zeta function regularization, see e.g. [9]. In the right plot of Fig. 2 we compare the numerical data to the prediction (5.5). For $M^2 R^2 \lesssim 5$ the data are in good agreement with F_{scalar} . For larger values of $M^2 R^2$ the error estimates grow rapidly, and there is no longer a meaningful comparison between the numerical data and F_{scalar} . The error estimates in the above plot, based on the extrapolation from $\Lambda R = 20$ to $\Lambda = \infty$, are clearly rather conservative.

Finally, we can compute the antipodal two-point function $\langle \phi(N)\phi(S) \rangle$ in the case of the ϕ^2 flow. In Fig. 3 we compare formula (5.2) to numerical data computed in our scheme. Since the correlator in question decays exponentially with MR , it is more convenient to plot the observable

$$f(MR) := \ln R^{d-2} \langle \phi(N)\phi(S) \rangle_{\text{conn}}$$

which decays linearly with MR . The plot in question is measured at cutoff $\Lambda R = 20$, and we have not extrapolated to $\Lambda = \infty$, contrary to the plots from Fig. 2; the error bars only reflect the extrapolation to $T = \infty$, cf. the discussion at the end of Sec. 5.1. Up to $M^2 R^2 \simeq 5$, we find excellent agreement between our data and the exact formula; for larger radii, it is necessary to use higher cutoffs.

¹³The same flow was recently discussed in [53] in the context of putative F -functions that monotonically interpolate between UV and IR fixed points.

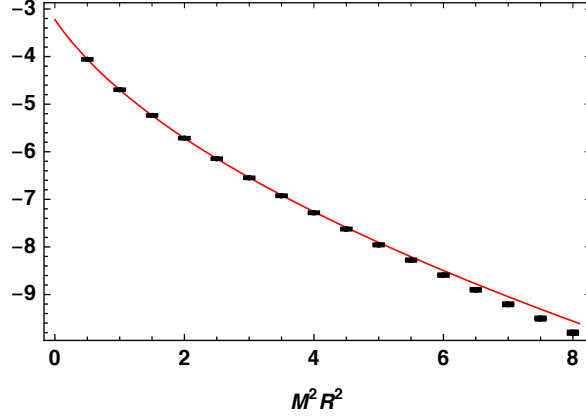


Figure 3: The logarithm of the correlator $\langle \phi(N)\phi(S) \rangle_{\text{conn}}$ in the presence of the $\frac{1}{2}M^2\phi^2$ flow, scanning over a range of couplings $M^2 R^2$ (horizontal axis) at cutoff $\Lambda R = 20$. Black dots with error bars: numerical data; red curve: exact result from Eq. (5.2).

5.3 Cubic interaction

Next, we consider a cubic interaction on S^3 with imaginary coupling

$$S_{\text{bare}} = S_0 + \frac{i\lambda}{3!} \int_{S^3} \sqrt{g} d^3x \phi^3(x) \quad (5.6)$$

again using the $m^2 = 0$ theory as a starting point. We will consider the following values of the coupling: $\bar{\lambda} \equiv \lambda R^{3/2} = \{0.1, 1, 2\}$, so we can test both the perturbative and the strong-coupling regime. As discussed at length in Sec. 4, the bare action is UV-divergent, whereas the renormalized action

$$S_{\text{ren}} = S_{\text{bare}} + \int_{S^3} \sqrt{g} d^3x \left[-\frac{\lambda^2}{192\pi^2} \ln(\Lambda/|\lambda|^{2/3}) + \frac{\lambda^2}{64\Lambda} \phi^2(x) \right] \quad (5.7)$$

is expected to have a well-defined continuum limit. We will test this prediction by scanning over a range of cutoffs, from $\Lambda R = 8$ to $\Lambda R = 18$. To be precise, we show plots of the quantity

$$h(\bar{\lambda}) := \bar{\lambda}^{-2} \ln \frac{Z(\lambda)}{Z(0)}$$

as a function of the cutoff Λ , computed for the two actions S_{bare} and S_{ren} , on the left (resp. right) side of Fig. 4. Indeed we observe that the bare partition function is divergent, whereas the free energy of the renormalized theory has a finite limit as $\Lambda \rightarrow \infty$ up to an error of $1/\Lambda$.

As in the case of the ϕ^2 flow, we also compute the antipodal correlation function $\langle \phi(N)\phi(S) \rangle_{\text{conn}}$. The results are shown in Fig. 5; we find that the measured correlator converges rapidly, roughly as $1/\Lambda^2$, to its value in the continuum limit. This observation is in agreement with the discussion from Sec. 4.4.¹⁴

¹⁴In Sec. 4.4 the presence of a spurious term vanishing as $1/\Lambda$ was mentioned. This term appears with a small coefficient, of order $10^{-2} \cdot \bar{\lambda}^2$ relative to the tree level contribution. For sufficiently large Λ , we therefore expect a $1/\Lambda$ decay of the truncation error. To properly analyze this issue, more data are needed.

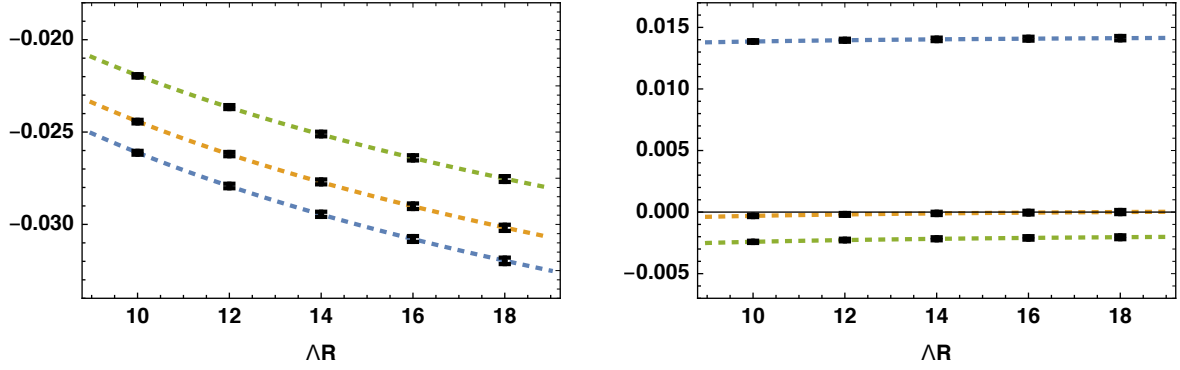


Figure 4: **Left:** Logarithm of the partition function $h(\bar{\lambda})$ for the bare action S_{bare} as a function of the cutoff ΛR (horizontal axis). Black dots with error bars: numerical data; dotted lines: logarithmic fits. The three curves correspond to different couplings $\bar{\lambda} = \{0.1, 1, 2\}$, shown in {blue, orange, green}. **Right:** same observable, computed for the renormalized action S_{ren} . The dotted lines now correspond to $1/\Lambda$ fits.

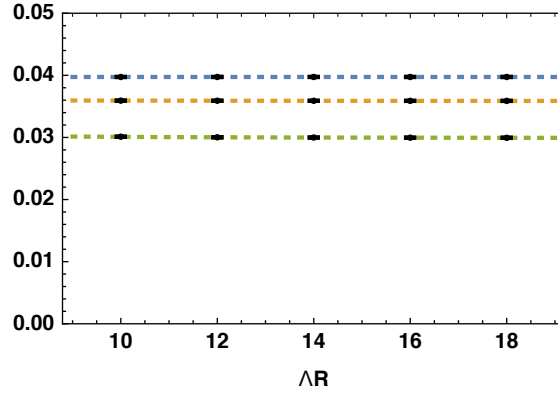


Figure 5: The antipodal correlator $R\langle\phi(N)\phi(S)\rangle$ for the cubic action S_{ren} as a function of the cutoff Λ (horizontal axis). The three different curves correspond to the different couplings $\bar{\lambda}$, see Fig. 4. Black points with error bars: numerical data. Dotted lines: $1/\Lambda^2$ fits.

6 Ward identities and one-point functions

The cutoff Λ used in our scheme breaks the full rotation symmetry $\text{SO}(d+1)$ of the d -sphere, although a subgroup $\text{SO}(d)$ of spatial rotations is preserved. This translates to violations of the Ward identities (2.5) at the cutoff scale. It is crucial that the full spacetime symmetry group is recovered in the limit $\Lambda \rightarrow \infty$. In many cases (e.g. lattice regularizations) the regulator used is *local*, and general RG arguments can be used to argue that spacetime symmetries are restored in the continuum limit. Unfortunately the regulator Λ is nonlocal, hence there is no simple classification of $\text{SO}(d+1)$ -violating counterterms. However, on a case-by-case basis we can measure violations of Ward identities to better understand the restoration of rotation invariance. In this section, we specialize to perhaps the simplest example, the one-point function of $\langle\phi^2(\tau, \mathbf{n})\rangle$ in the presence of quadratic and cubic interactions on S^3 , computing violations of the Ward identity to second order in perturbation theory.

6.1 Operator renormalization at leading order

As in Sec. 4.2, let's start by considering a general perturbation \mathcal{O} in d dimensions. The one-point function $\langle \mathcal{O}(\tau, \mathbf{n}) \rangle$ is generated at first order in the coupling λ , to wit

$$\langle \mathcal{O}(\tau, \mathbf{n}) \rangle = -\bar{\lambda} \int_{-\infty}^{\infty} \frac{d\tau'}{(\cosh \tau')^d} \langle \emptyset | T \mathcal{O}(\tau, \mathbf{n}) \hat{\mathcal{O}}(\tau') | \emptyset \rangle_0 + O(\lambda^2). \quad (6.1)$$

As discussed in Sec. 4.2, the $\langle \mathcal{O} \mathcal{O} \rangle_0$ correlator is non-universal, and to simplify the following computation we use the short-distance approximation introduced in Eq. (4.3). Using the same logic as in that section, we arrive at the following estimate for the VEV $\langle \mathcal{O} \rangle$:

$$\langle \mathcal{O}(\tau, \mathbf{n}) \rangle = -\frac{\bar{\lambda} a}{R^\Delta} \mathcal{V}(\tau, \Lambda) + \dots, \quad \mathcal{V}(\tau, \Lambda) = S_d \sum_{k=0}^{\Lambda R/2} \frac{(\Delta)_k (\Delta - d/2 + 1)_k}{k! (d/2)_k} (\cosh \tau)^\Delta \hat{G}_0(d - \Delta, \Delta + 2k | \tau). \quad (6.2)$$

Here \hat{G}_0 is a special function, defined in (B.4). The upper limit $k_{\max} = \Lambda R/2$ in (6.2) is a rough estimate, just as in Sec. 4.2, but it suffices since we are only interested in the leading scaling with Λ . For $\Delta < d/2$, the expansion (6.2) converges uniformly in τ , whereas for $\Delta \geq d/2$ it diverges, reflecting a UV divergence of the VEV $\langle \mathcal{O} \rangle$. Henceforth we will assume that $\Delta < d/2$.

We claim that the Ward identity for $\langle \mathcal{O} \rangle$ (which must be constant) is violated by effects of order $1/\Lambda^{d-2\Delta}$. To make this precise, we have to analyze the behaviour of $\mathcal{V}(\tau, \Lambda)$ at large Λ . This can be done using Eq. (B.3), which leads to the estimate

$$\mathcal{V}(\tau, \Lambda) = 2^{d-2\Delta-1} S_d B(\tfrac{1}{2}d - \Delta, \tfrac{1}{2}d) - \frac{\rho(\Delta)}{(\Lambda R \cosh \tau)^{d-2\Delta}} + O(1/\Lambda^{d-2\Delta+1}), \quad \rho(\Delta) = \frac{2^{d-2\Delta} \Gamma(\tfrac{1}{2}d)}{(d-2\Delta) \Gamma(\Delta) \Gamma(\Delta - \tfrac{1}{2}d + 1)}. \quad (6.3)$$

Indeed, the leading truncation error depends explicitly on τ . The above error term can be canceled by renormalizing the operator \mathcal{O} by a nonlocal counterterm. Indeed, suppose that we define a renormalized operator $\mathcal{O}_r(\tau, \mathbf{n})$ as follows:

$$\mathcal{O}(\tau, \mathbf{n}) =: \mathcal{O}_r(\tau, \mathbf{n}) + a\lambda \frac{\rho(\Delta)}{(\Lambda \cosh \tau)^{d-2\Delta}} \mathbb{1}. \quad (6.4)$$

Then it is easy to see $\langle \mathcal{O}_r(\tau, \mathbf{n}) \rangle$ will be less cutoff-sensitive, in the sense the error term of order $1/\Lambda^{d-2\Delta}$ in (6.3) will be absent. In principle it's possible to compute subleading truncation effects as well, but we have not done so in the present work.

6.2 (N)LO computation for $\langle \phi^2 \rangle$

We can test this prescription in the case of the $\phi^2 + \phi^3$ theory on S^3 , taking $\mathcal{O} = \phi^2$. To proceed, we compute the VEV $\langle \phi^2(\tau, \mathbf{n}) \rangle$ for the bare operator ϕ^2 using time-dependent perturbation theory, which yields

$$R^{d-2} \langle \phi^2(\tau, \mathbf{n}) \rangle_\Lambda = \bar{\lambda}_2 \mathcal{E}_{2,1}(\tau, \Lambda) + \bar{\lambda}_2^2 \mathcal{E}_{2,2}(\tau, \Lambda) + \bar{\lambda}_3^2 \mathcal{E}_{3,2}(\tau, \Lambda) + O(\lambda_2^3, \lambda_3^4) \quad (6.5)$$

for some functions $\mathcal{E}_{n,k}(\tau, \Lambda)$ that will be displayed later. Let us focus on the leading-order contribution:

$$\mathcal{E}_{2,1}(\tau, \Lambda) = -\frac{1}{S_d} \sum_{\ell} n_{\ell}^d \Theta(2\varepsilon(\ell) \leq \Lambda) \left[\int_{-\infty}^{\tau} \frac{d\tau'}{(\cosh \tau')^d} [K_{\ell}(\tau) K_{\ell}(-\tau')]^2 + (\tau \rightarrow -\tau) \right]. \quad (6.6)$$

According to the discussion from the previous section, we expect that $\mathcal{E}_{2,1}(\tau, \Lambda)$ depends on τ through effects of order $1/\Lambda^{d-2\Delta} = 1/\Lambda$. Moreover, Eq. (6.4) provides a quantitative prediction, namely that the VEV of the renormalized operator

$$d = 3 : \quad \phi_r^2 := \phi^2 - \frac{\lambda_2}{4\pi\Lambda \cosh \tau} \mathbb{1} \quad (6.7)$$

violates the Ward identity only through subleading effects of order $1/\Lambda^2$, at least to leading order in λ_2 . We have tested these predictions for the $m^2 = 0$ theory by evaluating the function (6.6) at large values of Λ . In Fig. 6 we compare the VEV of the bare operator ϕ^2 to the one of the renormalized operator ϕ_r^2 for two values of the cutoff Λ at first order in λ_2 . Although rotation-invariance breaking effects vanish as $1/\Lambda$, they are clearly observable for small values of Λ in the case of the bare operator. As expected, the plot shows that the nonlocal counterterm (6.7) captures most of the $\text{SO}(d+1)$ -breaking effects.

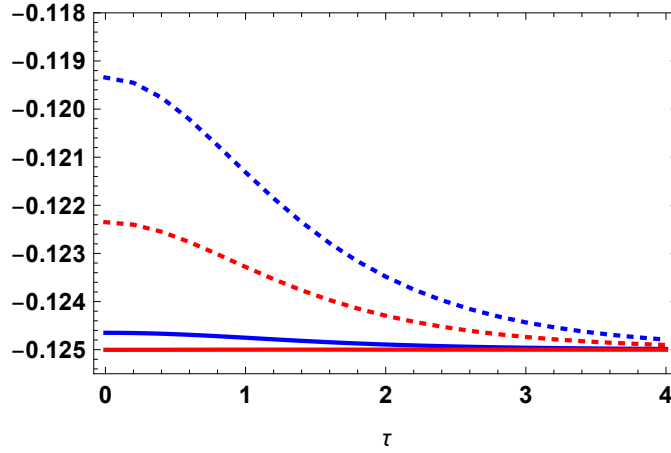


Figure 6: The leading-order contribution $\mathcal{E}_{2,1}$ to the VEV $\langle \phi^2(\tau) \rangle$ in the massless $3d$ theory, as a function of τ . We show the result for two different cutoffs: $\Lambda R = 15$ (blue) and $\Lambda R = 30$ (red). The dotted (resp. solid) line corresponds to VEV of the bare (renormalized) operator. The exact value of this diagram is $\mathcal{E}_{2,1}(\Lambda \rightarrow \infty) = -1/8$, see Eq. (4.1c).

The analysis in Sec. 6.1 only considered leading-order contributions to one-point functions. Nonetheless, by examining the two diagrams $\mathcal{E}_{n,2}$ from (6.5), we can learn something about Ward identity violations at subleading orders. The relevant contributions $\mathcal{E}_{n,2}(\tau, \Lambda)$ are slightly more complicated. There are two qualitatively different diagrams $\mathcal{E}^{(1,2)}$ that need to be taken into account, corresponding to different time-orderings:

$$\begin{aligned} \mathcal{E}_{n,2}^{(1)}(\tau, \Lambda) &= \frac{2n}{n!S_d} \sum \Theta(2\varepsilon(\ell) \leq \Lambda) \Theta(\varepsilon(\ell) + \varepsilon(j_1) + \dots + \varepsilon(j_{n-1}) \leq \Lambda) A_n(\ell, j_1, \dots, j_{n-1}) \\ &\times \left[K_\ell(\tau)^2 \int_{-\infty}^{\tau} \frac{d\sigma}{(\cosh \sigma)^d} \int_{-\infty}^{\sigma} \frac{d\sigma'}{(\cosh \sigma')^d} K_\ell(-\sigma) K_\ell(-\sigma') \prod_{i=1}^{n-1} K_{j_i}(\sigma) K_{j_i}(-\sigma') + (\tau \rightarrow -\tau) \right] \end{aligned} \quad (6.8a)$$

and

$$\begin{aligned} \mathcal{E}_{n,2}^{(2)}(\tau, \Lambda) &= \frac{2n}{n!S_d} \sum \Theta(\varepsilon(\ell) + \varepsilon(j_1) + \dots + \varepsilon(j_{n-1}) \leq \Lambda) A_n(\ell, j_1, \dots, j_{n-1}) \\ &\times K_\ell(\tau) K_\ell(-\tau) \int_\tau^\infty \frac{d\sigma}{(\cosh \sigma)^d} \int_{-\infty}^\tau \frac{d\sigma'}{(\cosh \sigma')^d} K_\ell(\sigma) K_\ell(-\sigma') \prod_{i=1}^{n-1} K_{j_i}(\sigma) K_{j_i}(-\sigma'). \end{aligned} \quad (6.8b)$$

In both expressions, the sum runs over all tuples $\{\ell, j_1, \dots, j_{n-1}\}$. The above expression does not take into account the RG-improvement counterterm (4.31) that is generated at order λ_3^2 . Adding this counterterm to the action, the function $\mathcal{E}_{3,2}(\tau, \Lambda)$ shifts as

$$\mathcal{E}_{3,2}(\tau, \Lambda) \longrightarrow \mathcal{E}_{3,2}(\tau, \Lambda) + \frac{1}{4 \cdot 64 \cdot \Lambda R} + O(1/\Lambda^2). \quad (6.9)$$

Let us discuss the quadratic and cubic interactions separately, starting with the quadratic ($n = 2$) one. By numerically evaluating the diagram $\mathcal{E}_{2,2}$, we find that rotation-invariance violation effects are of the order of $1/\Lambda^3$:

$$\mathcal{E}_{2,2}(\tau, \Lambda) = \frac{1}{8} - \frac{f_2(\tau)}{(\Lambda R)^3} + O(1/\Lambda^4) \quad (6.10)$$

for some function $f_2(\tau)$. Since truncation error scales as $1/\Lambda^3$, it is negligible even for moderate values of the cutoff, and we have not attempted to compute the function $f_2(\tau)$.

The convergence of the cubic ($n = 3$) term with Λ is much slower. A numerical analysis of $\mathcal{E}_{3,2}$ shows that there is a residual truncation error of order $1/\Lambda$, contrary to the $1/\Lambda^3$ scaling in the quadratic case. In principle, we could further renormalize the operator ϕ^2 by adding an additional nonlocal counterterm

$$\phi_{\mathbf{r}}^2(\tau, \mathbf{n}) \mapsto \phi_{\mathbf{r}}^2(\tau, \mathbf{n}) + \frac{\lambda_3^2 R}{\Lambda} f_3(\tau) \mathbb{1} \quad (6.11)$$

to cancel these $1/\Lambda$ rotation-invariance breaking effects. Determining the function $f_3(\tau)$ is however a difficult exercise that will be left for future work.

7 Discussion

In this paper we developed a new framework to perform QFT computations on the d -dimensional sphere. In the case of the ϕ^2 flow in $d = 3$, we found good agreement between the data computed in our scheme and analytic results. For the $i\phi^3$ flow on S^3 , we provided strong numerical evidence that the theory is UV-finite after adding a local counterterm that grows logarithmically with the cutoff Λ . Finally, we analyzed the violation of $\text{SO}(d+1)$ Ward identities in the case of the one-point function $\langle \phi^2 \rangle$ on S^3 in perturbation theory, and showed that such violations vanish in the continuum limit $\Lambda \rightarrow \infty$.

It is an outstanding problem to compute the F -coefficient for nontrivial $3d$ CFTs, like the Ising or Lee-Yang theories, to high precision. This requires performing a finetuning in the UV (in order to reach the critical point) and computing the partition function $Z(R)$ for a range of radii $R \gg 1$, in order to subtract the two curvature counterterms from Eq. (1.1). An estimate of F for the $3d$ Ising model, obtained using the epsilon expansion, was given in [12]. We are not aware of any published estimate of F for the Lee-Yang CFT. Moreover, it would be interesting to compare integrated correlation functions for the $3d$ Ising model on S^3 to recent predictions for Binder cumulants from Ref. [54].

Although we specialized to scalar quantum field theories on S^d , our approach is rather general. It is completely straightforward to extend the same method to theories with fermions. Moreover, the

S^d geometry only featured in two places: through the mode functions $K_\ell(\tau)$ that appeared in the quantization of ϕ , and via a factor $1/(\cosh \tau)^d$ appearing in the Dyson operator (3.8). The same method can be adapted to any manifold that is Weyl-equivalent to $\mathbb{R} \times S^{d-1}$. Examples of such manifolds are Euclidean anti-de Sitter space (in the Poincaré disk picture), flat space and de Sitter space. In the case of de Sitter space, the quantization in question was recently used in Ref. [55], which studied the large- N limit of the $O(N)$ fixed point on dS_3 using gap equations.

The truncation procedure used in this work was chosen more or less ad hoc, and it seems worthwhile to examine whether a different truncation might be more efficient. Moreover, we evaluated matrix elements of the Dyson operator U explicitly, by dividing the sphere into $T \gg 1$ timeslices and summing over all intermediate states. This is numerically inexpensive for small cutoffs of order $\Lambda R \sim 10 - 20$, but the exponential growth of the Fock space with Λ means that cutoffs beyond $\Lambda R \sim 30 - 40$ are not easily accessible. To obtain precise results, it is therefore crucial to compute further RG-improvement counterterms, for instance those of order $1/\Lambda^2$.

We did not use any CFT techniques in our numerical computations, although the UV theory used was conformally invariant (having $m^2 = 0$). We believe that conformal symmetry could be a powerful tool to improve our approach. For one, it completely fixes the matrix elements $\langle \psi_i | \widehat{\phi}^n(\tau) | \psi_j \rangle$ in terms of a small number of OPE coefficients. The next-to-leading term in the expansion of the Dyson operator is an integral over a matrix element of the form

$$\langle \psi_i | \widehat{\phi}^n(\tau) \widehat{\phi}^{n'}(\tau') | \psi_j \rangle. \quad (7.1)$$

Such integrals can be estimated accurately by interpreting (7.1) as a CFT four-point function, expanding the latter into conformal blocks and summing over all descendants. Taking such CFT ideas into account, it seems possible to increase the cutoff and simultaneously reduce the computational cost (the number T of timeslices).

As a final comment, we mention that in earlier work on so-called spherical or modal field theory a stochastic technique (diffusion Monte Carlo) was used to compute a similar quantity, namely a transition amplitude on $\mathbb{R} \times S^1$ [56] resp. $\mathbb{R} \times S^2$ [57]. It would be interesting to compare both methods, or perhaps to apply an entirely different numerical approach to our problem.

Acknowledgements

This research was supported in part by Perimeter Institute for Theoretical Physics. Research at Perimeter Institute is supported by the Government of Canada through the Department of Innovation, Science and Economic Development Canada and by the Province of Ontario through the Ministry of Research, Innovation and Science. The author thanks Freddy Cachazo, Jaume Gomis, Niamh Maher, Lorenzo di Pietro, Silviu Pufu, Leonardo Rastelli, Slava Rychkov and Balt van Rees for discussions or comments, and Slava Rychkov for comments on the manuscript.

References

- [1] Al. B. Zamolodchikov, “Scaling Lee-Yang model on a sphere. 1. Partition function,” *JHEP* **07** (2002) 029, [arXiv:hep-th/0109078](#) [[hep-th](#)].
- [2] A. Zamolodchikov, “Irreversibility of the Flux of the Renormalization Group in a 2D Field Theory,” *JETP Lett.* **43** (1986) 730–732.
- [3] J. L. Cardy, “Is there a c -theorem in four dimensions?,” *Phys. Lett.* **B215** (1988) 749–752.
- [4] H. Casini and M. Huerta, “On the RG running of the entanglement entropy of a circle,” *Phys. Rev.* **D85** (2012) 125016, [arXiv:1202.5650](#) [[hep-th](#)].

- [5] H. Liu and M. Mezei, “A Refinement of entanglement entropy and the number of degrees of freedom,” *JHEP* **04** (2013) 162, [arXiv:1202.2070 \[hep-th\]](#).
- [6] I. R. Klebanov, T. Nishioka, S. S. Pufu, and B. R. Safdi, “Is Renormalized Entanglement Entropy Stationary at RG Fixed Points?,” *JHEP* **10** (2012) 058, [arXiv:1207.3360 \[hep-th\]](#).
- [7] H. Casini, M. Huerta, R. C. Myers, and A. Yale, “Mutual information and the F -theorem,” *JHEP* **10** (2015) 003, [arXiv:1506.06195 \[hep-th\]](#).
- [8] O. Ben-Ami, D. Carmi, and M. Smolkin, “Renormalization group flow of entanglement entropy on spheres,” *JHEP* **08** (2015) 048, [arXiv:1504.00913 \[hep-th\]](#).
- [9] I. R. Klebanov, S. S. Pufu, and B. R. Safdi, “ F -Theorem without Supersymmetry,” *JHEP* **10** (2011) 038, [arXiv:1105.4598 \[hep-th\]](#).
- [10] D. Anninos, F. Denef, and D. Harlow, “Wave function of Vasiliev’s universe: A few slices thereof,” *Phys. Rev.* **D88** no. 8, (2013) 084049, [arXiv:1207.5517 \[hep-th\]](#).
- [11] L. Fei, S. Giombi, and I. R. Klebanov, “Critical $O(N)$ models in $6 - \epsilon$ dimensions,” *Phys. Rev.* **D90** no. 2, (2014) 025018, [arXiv:1404.1094 \[hep-th\]](#).
- [12] S. Giombi and I. R. Klebanov, “Interpolating between a and F ,” *JHEP* **03** (2015) 117, [arXiv:1409.1937 \[hep-th\]](#).
- [13] L. Fei, S. Giombi, I. R. Klebanov, and G. Tarnopolsky, “Generalized F -Theorem and the ϵ Expansion,” *JHEP* **12** (2015) 155, [arXiv:1507.01960 \[hep-th\]](#).
- [14] S. Giombi, I. R. Klebanov, and G. Tarnopolsky, “Conformal QED_d, F -Theorem and the ϵ Expansion,” *J. Phys.* **A49** no. 13, (2016) 135403, [arXiv:1508.06354 \[hep-th\]](#).
- [15] G. Tarnopolsky, “Large N expansion of the sphere free energy,” *Phys. Rev.* **D96** no. 2, (2017) 025017, [arXiv:1609.09113 \[hep-th\]](#).
- [16] D. L. Jafferis, “The Exact Superconformal R-Symmetry Extremizes Z ,” *JHEP* **05** (2012) 159, [arXiv:1012.3210 \[hep-th\]](#).
- [17] D. L. Jafferis, I. R. Klebanov, S. S. Pufu, and B. R. Safdi, “Towards the F -Theorem: $\mathcal{N} = 2$ Field Theories on the Three-Sphere,” *JHEP* **06** (2011) 102, [arXiv:1103.1181 \[hep-th\]](#).
- [18] D. R. Gulotta, C. P. Herzog, and S. S. Pufu, “From Necklace Quivers to the F -theorem, Operator Counting, and $T(U(N))$,” *JHEP* **12** (2011) 077, [arXiv:1105.2817 \[hep-th\]](#).
- [19] C. Closset, T. T. Dumitrescu, G. Festuccia, Z. Komargodski, and N. Seiberg, “Contact Terms, Unitarity, and F -Maximization in Three-Dimensional Superconformal Theories,” *JHEP* **10** (2012) 053, [arXiv:1205.4142 \[hep-th\]](#).
- [20] Z. Komargodski, “Aspects of Renormalization Group Flows.” <http://goo.gl/kKdoJb>.
- [21] R. C. Brower, G. Fleming, A. Gasbarro, T. Raben, C.-I. Tan, and E. Weinberg, “Quantum Finite Elements for Lattice Field Theory,” *PoS LATTICE2015* (2016) 296, [arXiv:1601.01367 \[hep-lat\]](#).
- [22] R. C. Brower, E. S. Weinberg, G. T. Fleming, A. D. Gasbarro, T. G. Raben, and C.-I. Tan, “Lattice Dirac Fermions on a Simplicial Riemannian Manifold,” *Phys. Rev.* **D95** no. 11, (2017) 114510, [arXiv:1610.08587 \[hep-lat\]](#).
- [23] R. C. Brower, M. Cheng, E. S. Weinberg, G. T. Fleming, A. D. Gasbarro, T. G. Raben, and C.-I. Tan, “Lattice ϕ^4 field theory on Riemann manifolds: Numerical tests for the 2-d Ising CFT on \mathbb{S}^2 ,” *Phys. Rev.* **D98** no. 1, (2018) 014502, [arXiv:1803.08512 \[hep-lat\]](#).
- [24] R. C. Brower, G. T. Fleming, and H. Neuberger, “Lattice Radial Quantization: 3D Ising,” *Phys. Lett.* **B721** (2013) 299–305, [arXiv:1212.6190 \[hep-lat\]](#).
- [25] R. C. Brower, G. T. Fleming, and H. Neuberger, “Radial Quantization for Conformal Field Theories on the Lattice,” *PoS LATTICE2012* (2012) 061, [arXiv:1212.1757 \[hep-lat\]](#).
- [26] R. C. Brower, M. Cheng, and G. T. Fleming, “Improved Lattice Radial Quantization,” *PoS LATTICE2013* (2014) 335, [arXiv:1407.7597 \[hep-lat\]](#).

- [27] A. J. A. James, R. M. Konik, P. Lecheminant, N. J. Robinson, and A. M. Tsvelik, “Non-perturbative methodologies for low-dimensional strongly-correlated systems: From non-abelian bosonization to truncated spectrum methods,” *Rept. Prog. Phys.* **81** no. 4, (2018) 046002, [arXiv:1703.08421 \[cond-mat.str-el\]](#).
- [28] E. Katz, G. Marques Tavares, and Y. Xu, “Solving 2D QCD with an adjoint fermion analytically,” *JHEP* **05** (2014) 143, [arXiv:1308.4980 \[hep-th\]](#).
- [29] M. Hogervorst, S. Rychkov, and B. C. van Rees, “Truncated conformal space approach in d dimensions: A cheap alternative to lattice field theory?,” *Phys. Rev.* **D91** (2015) 025005, [arXiv:1409.1581 \[hep-th\]](#).
- [30] E. Katz, G. Marques Tavares, and Y. Xu, “A solution of 2D QCD at Finite N using a conformal basis,” [arXiv:1405.6727 \[hep-th\]](#).
- [31] S. Rychkov and L. G. Vitale, “Hamiltonian truncation study of the ϕ^4 theory in two dimensions,” *Phys. Rev.* **D91** (2015) 085011, [arXiv:1412.3460 \[hep-th\]](#).
- [32] S. Rychkov and L. G. Vitale, “Hamiltonian truncation study of the ϕ^4 theory in two dimensions. II. The \mathbb{Z}_2 -broken phase and the Chang duality,” *Phys. Rev.* **D93** no. 6, (2016) 065014, [arXiv:1512.00493 \[hep-th\]](#).
- [33] J. Elias-Miro, M. Montull, and M. Riembau, “The renormalized Hamiltonian truncation method in the large E_T expansion,” *JHEP* **04** (2016) 144, [arXiv:1512.05746 \[hep-th\]](#).
- [34] E. Katz, Z. U. Khandker, and M. T. Walters, “A Conformal Truncation Framework for Infinite-Volume Dynamics,” *JHEP* **07** (2016) 140, [arXiv:1604.01766 \[hep-th\]](#).
- [35] B. Balthazar, V. A. Rodriguez, and X. Yin, “Hamiltonian Truncation Study of Supersymmetric Quantum Mechanics: S-Matrix and Metastable States,” [arXiv:1610.07275 \[hep-th\]](#).
- [36] J. Elias-Miro, S. Rychkov, and L. G. Vitale, “NLO Renormalization in the Hamiltonian Truncation,” *Phys. Rev.* **D96** no. 6, (2017) 065024, [arXiv:1706.09929 \[hep-th\]](#).
- [37] J. Elias-Miro, S. Rychkov, and L. G. Vitale, “High-Precision Calculations in Strongly Coupled Quantum Field Theory with Next-to-Leading-Order Renormalized Hamiltonian Truncation,” *JHEP* **10** (2017) 213, [arXiv:1706.06121 \[hep-th\]](#).
- [38] S. Whitsitt, M. Schuler, L.-P. Henry, A. M. Läuchli, and S. Sachdev, “Spectrum of the Wilson-Fisher conformal field theory on the torus,” *Phys. Rev.* **B96** no. 3, (2017) 035142, [arXiv:1701.03111 \[cond-mat.str-el\]](#).
- [39] N. Anand, V. X. Genest, E. Katz, Z. U. Khandker, and M. T. Walters, “RG flow from ϕ^4 theory to the 2D Ising model,” *JHEP* **08** (2017) 056, [arXiv:1704.04500 \[hep-th\]](#).
- [40] D. Rutter and B. C. van Rees, “Counterterms in Truncated Conformal Perturbation Theory,” [arXiv:1803.05798 \[hep-th\]](#).
- [41] A. L. Fitzpatrick, J. Kaplan, E. Katz, L. G. Vitale, and M. T. Walters, “Lightcone effective Hamiltonians and RG flows,” *JHEP* **08** (2018) 120, [arXiv:1803.10793 \[hep-th\]](#).
- [42] C. M. Bender, V. Branchina, and E. Messina, “Ordinary versus PT-symmetric ϕ^3 quantum field theory,” *Phys. Rev.* **D85** (2012) 085001, [arXiv:1201.1244 \[hep-th\]](#).
- [43] K. Atkinson and W. Han, *Spherical Harmonics and Approximations on the Unit Sphere: An Introduction*. Springer, 2012.
- [44] H. Osborn and G. M. Shore, “Correlation functions of the energy momentum tensor on spaces of constant curvature,” *Nucl. Phys.* **B571** (2000) 287–357, [arXiv:hep-th/9909043 \[hep-th\]](#).
- [45] N. Birrell and P. Davies, *Quantum Fields in Curved Space*. Cambridge University Press, 1982.
- [46] B. Simon, *Functional Integration and Quantum Physics*. AMS Chelsea Publishing, 2005.
- [47] Al. B. Zamolodchikov, “Perturbed conformal field theory on a sphere,” in *Statistical Field Theories*, A. Cappelli and G. Mussardo, eds., pp. 105–116. Springer, 2002.
- [48] P. Grinza and N. Magnoli, “On the magnetic perturbation of the Ising model on the sphere,” *J. Phys.* **A36** (2003) L509–L516, [arXiv:hep-th/0306100 \[hep-th\]](#).

- [49] S. Rychkov, *EPFL Lectures on Conformal Field Theory in $D \geq 3$ Dimensions*. SpringerBriefs in Physics. 2016. [arXiv:1601.05000](#) [[hep-th](#)].
- [50] D. Simmons-Duffin, “The Conformal Bootstrap,” in *Proceedings, Theoretical Advanced Study Institute in Elementary Particle Physics: New Frontiers in Fields and Strings (TASI 2015): Boulder, CO, USA, June 1-26, 2015*, pp. 1–74. 2017. [arXiv:1602.07982](#) [[hep-th](#)].
- [51] K. Symanzik, “Continuum Limit and Improved Action in Lattice Theories. 1. Principles and ϕ^4 Theory,” *Nucl.Phys.* **B226** (1983) 187.
- [52] P. Giokas and G. Watts, “The renormalisation group for the truncated conformal space approach on the cylinder,” [arXiv:1106.2448](#) [[hep-th](#)].
- [53] J. K. Ghosh, E. Kiritsis, F. Nitti, and L. T. Witkowski, “Holographic RG flows on curved manifolds and the F -theorem,” [arXiv:1810.12318](#) [[hep-th](#)].
- [54] D. Berkowitz, “Conformal invariance and the Ising model on a 3 sphere in connection with the Quantum Elemental Method,” [arXiv:1808.05862](#) [[hep-th](#)].
- [55] S. P. Kumar and V. Vaganov, “Nonequilibrium dynamics of the $O(N)$ model on dS_3 and AdS crunches,” *JHEP* **03** (2018) 092, [arXiv:1802.08202](#) [[hep-th](#)].
- [56] P. J. Marrero, E. A. Roura, and D. Lee, “A nonperturbative analysis of symmetry breaking in two-dimensional ϕ^4 theory using periodic field methods,” *Phys. Lett.* **B471** (1999) 45, [arXiv:hep-th/9906189](#) [[hep-th](#)].
- [57] M. Windolowski, “A Nonperturbative study of three-dimensional ϕ^4 theory,” [arXiv:hep-th/0002243](#) [[hep-th](#)].
- [58] J. Fuchs and C. Schweigert, *Symmetries, Lie Algebras and Representations*. Cambridge University Press, 2003.

A Spherical harmonics and Gegenbauer polynomials

We will employ the usual normalization for the spherical harmonics:

$$\int_{S^{d-1}} d\mathbf{n} Y_{\ell j}^*(\mathbf{n}) Y_{\ell' j'}(\mathbf{n}) = \delta_{\ell\ell'} \delta_{jj'}. \quad (\text{A.1})$$

As is clear from (A.1), the harmonics corresponding to a given spin ℓ are only fixed up to a unitary change of basis:

$$Y_{\ell j}(\mathbf{n}) \mapsto \sum_{j'} M_j^{j'} Y_{\ell j'}(\mathbf{n}), \quad M^\dagger = M^{-1}. \quad (\text{A.2})$$

Such a change of basis does not influence any physical results.

An important role will be played by the Gegenbauer polynomials $C_\ell^d(z)$, which we normalize such that $C_\ell^d(1) = 1$. Concretely, the $C_\ell^d(z)$ can be defined using a generating function

$$\frac{1}{(1 - 2zt + t^2)^{\frac{1}{2}d-1}} = \sum_{\ell=0}^{\infty} t^\ell \frac{(d-2)_\ell}{\ell!} C_\ell^d(z) \quad (\text{A.3})$$

and they are orthonormal in the following sense:

$$\frac{n_\ell^d \cdot S_{d-1}}{S_d} \int_{-1}^1 dz (1 - z^2)^{\frac{1}{2}(d-3)} C_\ell^d(z) C_{\ell'}^d(z) = \delta_{\ell\ell'}. \quad (\text{A.4})$$

The spherical harmonics are related to Gegenbauer polynomials via the so-called addition theorem:

$$\sum_{j=1}^{n_\ell^d} Y_{\ell j}^*(\mathbf{m}) Y_{\ell j}(\mathbf{n}) = \frac{n_\ell^d}{S_d} C_\ell^d(\mathbf{m} \cdot \mathbf{n}). \quad (\text{A.5})$$

Although the $Y_{\ell j}(\mathbf{n})$ appearing on the LHS depend on a choice of basis, the RHS does not. Note that in $d = 3$, we simply have $C_\ell^3(z) = \text{LegendreP}_\ell(z)$.

Next, let us consider the computation of various spherical integrals. A fundamental identity, which slightly generalizes Eq. (A.4), reads

$$\frac{n_\ell^d}{S_d} \int_{S^{d-1}} d\mathbf{m} C_\ell^d(\mathbf{m} \cdot \mathbf{n}_1) C_{\ell'}^d(\mathbf{m} \cdot \mathbf{n}_2) = \delta_{\ell\ell'} C_\ell^d(\mathbf{n}_1 \cdot \mathbf{n}_2). \quad (\text{A.6})$$

This can be proven either via (A.5) or by means of the identity

$$\int_{S^{d-1}} d\mathbf{n} f(\mathbf{m} \cdot \mathbf{n}) = S_{d-1} \int_{-1}^1 dz (1 - z^2)^{\frac{1}{2}(d-3)} f(z), \quad |\mathbf{m}| = 1. \quad (\text{A.7})$$

Next, let us consider the $A_n(\ell_1, \dots, \ell_n)$ integrals, defined in Eq. (4.14). For $n = 2$ the result follows immediately from (A.6), namely

$$A_2(\ell_1, \ell_2) = \delta_{\ell_1 \ell_2} n_\ell^d. \quad (\text{A.8})$$

For $n = 3$, we first rewrite the integral as

$$A_3(\ell_1, \ell_2, \ell_3) = n_{\ell_1}^d n_{\ell_2}^d n_{\ell_3}^d \frac{S_{d-1}}{S_d^2} \int_{-1}^1 dx (1 - x^2)^{\frac{1}{2}(d-3)} C_{\ell_1}^d(x) C_{\ell_2}^d(x) C_{\ell_3}^d(x) \quad (\text{A.9})$$

using (A.7). The above integral vanishes either if $\ell_1 + \ell_2 + \ell_3$ is odd, or if the triplet $\{\ell_1, \ell_2, \ell_3\}$ does not obey the triangle inequality. If both conditions are fulfilled, the result can be stated as

$$A_3(\ell_1, \ell_2, \ell_3) = \frac{(d-2)_\lambda}{S_d (\frac{1}{2}d)_\lambda (\frac{1}{2}d-1)^3} \prod_{i=1}^3 (\ell_i + \frac{1}{2}d-1) \frac{(\frac{1}{2}d-1)_{\lambda-\ell_i}}{(\lambda-\ell_i)!}, \quad \lambda = \frac{1}{2}(\ell_1 + \ell_2 + \ell_3). \quad (\text{A.10})$$

B Massless integrals

In the massless limit, the $K_\ell(\tau)$ functions simplify in the following way:

$$K_\ell(\tau) = \frac{1}{\sqrt{2\ell+d-2}} e^{-(\ell+\frac{1}{2}d-1)\tau} (\cosh \tau)^{\frac{1}{2}d-1} + O(m^2 R^2). \quad (\text{B.1})$$

This allows for the exact computation of various quantities in the limit $m^2 \rightarrow 0$, which we make use of in Sec. 4. As a starting point, let's consider the integral

$$\Re(\alpha + \beta) > 0: \quad G_0(\alpha, \beta|\tau) := \int_{-\infty}^{\tau} \frac{d\tau'}{(\cosh \tau')^\alpha} e^{-\beta(\tau-\tau')} \quad (\text{B.2a})$$

$$= \frac{\Gamma(\frac{1}{2}(\alpha + \beta))}{2(\cosh \tau)^\alpha} {}_2\tilde{F}_1 \left[\begin{matrix} 1, \alpha \\ 1 + \frac{1}{2}(\alpha + \beta) \end{matrix} \middle| \frac{e^\tau}{2 \cosh \tau} \right] \quad (\text{B.2b})$$

where ${}_p\tilde{F}_q$ denotes the regularized hypergeometric function. To prove the above identity, one can e.g. notice that (B.2b) is the unique solution to the first-order differential equation

$$\left[\beta + \frac{d}{d\tau} \right] G_0(\alpha, \beta|\tau) = \frac{1}{(\cosh \tau)^\alpha}$$

which satisfies $\lim_{\tau \rightarrow -\infty} G_0(\alpha, \beta|\tau) = 0$. At large β , keeping α and τ fixed, we have

$$G_0(\alpha, \beta|\tau) \underset{\beta \rightarrow \infty}{\sim} \frac{1}{(\cosh \tau)^\alpha \beta} + O(1/\beta^2). \quad (\text{B.3})$$

A similar integral is

$$\widehat{G}_0(\alpha, \beta|\tau) := \int_{-\infty}^{\infty} \frac{d\tau'}{(\cosh \tau')^\alpha} e^{-\beta|\tau-\tau'|} = G_0(\alpha, \beta|\tau) + G_0(\alpha, \beta|-\tau). \quad (\text{B.4})$$

For second-order corrections to the partition function, we need

$$G_1(\alpha, \beta) := \int_{-\infty}^{\infty} \frac{d\tau}{(\cosh \tau)^\alpha} \int_{-\infty}^{\tau} \frac{d\tau'}{(\cosh \tau')^\alpha} e^{-\beta(\tau-\tau')} \quad (\text{B.5a})$$

which converges if $\Re(\alpha + \beta) > 0$ as well as $\Re(\alpha) > 0$. Using Eq. (B.2b), it can be shown that the above integral evaluates to

$$G_1(\alpha, \beta) = 4^{\alpha-1} \Gamma(\alpha)^2 \Gamma\left(\frac{1}{2}(\alpha + \beta)\right) {}_3\widetilde{F}_2 \left[\begin{matrix} 1, \alpha, \alpha \\ 2\alpha, 1 + \frac{1}{2}(\alpha + \beta) \end{matrix} \middle| 1 \right]. \quad (\text{B.5b})$$

In the limit where $\beta \gg 1$ but α is kept fixed, we have

$$G_1(\alpha, \beta) \underset{\beta \rightarrow \infty}{\sim} \beta^{-1} B(\alpha, \tfrac{1}{2}) + O(1/\beta^2). \quad (\text{B.6})$$

C Additional comments about the algorithm

In Sec. 5.1, a brief description of the algorithm used in our work was given. In what follows, we will discuss three additional points that may be helpful for readers who want to implement a version of the algorithm themselves.

Our first comment involves generating a list of scalar states $|\psi_i\rangle$. Such states can be written as linear combinations of parity-even states with $L_z = 0$, which can be denoted as $|\chi_\alpha\rangle$. Schematically

$$|\psi_i\rangle = \sum_{\alpha} C_i^{\alpha} |\chi_{\alpha}\rangle \quad (\text{C.1})$$

for some matrix C with real-valued matrix elements. In principle, the matrix C can be computed by requiring that $L_{\pm}|\psi_i\rangle = 0$ — it's the kernel of either of the operators L_+ or L_- . Alternatively, the matrix C_i^{α} can be constructed using $\text{SO}(3)$ Lie algebra techniques. Working in a basis of states $|\chi_{\alpha}\rangle$ defined in Eq. (3.14), every line of the matrix C_i^{α} has a group-theoretical interpretation as a tensor T in a tensor product of $\text{SO}(3)$ representations. We can therefore generate scalar states by writing down manifestly invariant tensors, using Clebsch-Gordan coefficients and $3j$ symbols [58]. For instance, given three spins ℓ_i that obey the triangle equality and sum to an even integer, there is a unique scalar state:

$$\sum_{m_i} \begin{pmatrix} \ell_1 & \ell_2 & \ell_3 \\ m_1 & m_2 & m_3 \end{pmatrix} a_{\ell_1 m_1}^{\dagger} a_{\ell_2 m_2}^{\dagger} a_{\ell_3 m_3}^{\dagger} |\emptyset\rangle. \quad (\text{C.2})$$

The generalization to n -particle states is straightforward. In our experience, such a group-theoretical approach is faster than computing the kernel of L_{\pm} .

Second, we proceed by computing the matrix elements of $\widehat{\phi}_n(\tau)$ in a basis of the $|\chi_{\alpha}\rangle$ states and restricting to scalar states later on. For simplicity, let's work in a basis where $\langle\psi_i|\psi_j\rangle = \delta_{ij}$ and $\langle\chi_{\alpha}|\chi_{\beta}\rangle = \delta_{\alpha\beta}$, which implies that

$$C \cdot {}^t C = \mathbb{1}. \quad (\text{C.3})$$

Although it is easy to orthonormalize the states $|\chi_{\alpha}\rangle$, making the scalars $|\psi_i\rangle$ orthonormal requires the use of the Gram-Schmidt procedure, which is somewhat expensive. Let

$$[W_n(\tau)]^{\alpha}_{\beta} = [W_n(\tau)]_{\alpha\beta} := \langle\chi_{\alpha}|\widehat{\phi}_n(\tau)|\chi_{\beta}\rangle. \quad (\text{C.4})$$

Using (C.1) it follows that

$$[V_n(\tau)]_j^i = [V_n(\tau)]_{ij} = [C \cdot W_n(\tau) \cdot {}^t C]_{ij}. \quad (\text{C.5})$$

The matrices $W_n(\tau)$ are rather large — for $\Lambda R = 20$, they have 166802×166802 entries, see Table 1. Using an additional trick, the dimension of W_n can be reduced, as is explained in the final paragraph of this section. Next, notice that hermiticity puts constraints on the matrices V_n and W_n , namely

$$[V_n(\tau)]_{ij} = [V_n(-\tau)]_{ji} \quad \text{and} \quad [W_n(\tau)]_{\alpha\beta} = [W_n(-\tau)]_{\beta\alpha}. \quad (\text{C.6})$$

A second consistency condition follows from rotation invariance. Let \mathcal{P} be the operator that projects onto scalar states:

$$\mathcal{P} = \sum_{\alpha\beta} [{}^t C \cdot C]^{\alpha\beta} |\chi_\alpha\rangle\langle\chi_\beta|, \quad \mathcal{P}^2 = \mathcal{P}. \quad (\text{C.7})$$

The rotation invariance of $\widehat{\phi^n}(\tau)$ implies that

$$\forall i : \quad \mathcal{P} \widehat{\phi^n}(\tau) |\psi_i\rangle = \widehat{\phi^n}(\tau) |\psi_i\rangle, \quad (\text{C.8})$$

which translates to the matrix constraint

$${}^t C \cdot V_n(\tau) = W_n(\tau) \cdot {}^t C. \quad (\text{C.9})$$

If Eq. (C.9) is not satisfied, at least one matrix element of $W_n(\tau)$ or $V_n(\tau)$ must be incorrect.

Finally, we point out a trick that can be used to drastically simplify the computation of matrix elements. The key idea is that a basis state $|\chi_\alpha\rangle$ can always be written in the following form:

$$|\chi_\alpha\rangle = \frac{1}{\sqrt{k_\alpha!}} (a_{0,0}^\dagger)^{k_\alpha} |\xi_\alpha\rangle \quad (\text{C.10})$$

for some integer $k_\alpha \geq 0$, where $|\xi_\alpha\rangle$ is a state without $a_{0,0}^\dagger$ creation operators. We claim that the matrix $W_n(\tau)$ can be expressed in terms of matrix elements of the form $\langle\xi_\alpha|\widehat{\phi^{n'}}(\tau)|\xi_\beta\rangle$ for $1 \leq n' \leq n$. This is a simple consequence of the operator identity

$$[\widehat{\phi^n}(\tau), a_{0,0}^\dagger] = \frac{n}{\sqrt{S_d}} K_0(\tau) \widehat{\phi^{n-1}}(\tau), \quad (\text{C.11})$$

using the convention $\widehat{\phi^0}(\tau) = S_d \mathbb{1}$. The proof of Eq. (C.11) is left to the reader.